In presenting this dissertation as a partial fulfillment of the requirements for an advanced degree from the Georgia Institute of Technology, I agree that the Library of the Institution shall make it available for inspection and circulation in accordance with its regulations governing materials of this type. I agree that permission to copy from, or to publish from, this dissertation may be granted by the professor under whose direction it was written, or, in his absence, by the Dean of the Graduate Division when such copying or publication is solely for scholarly purposes and does not involve potential financial gain. It is understood that any copying from, or publication of, this dissertation which involves potential financial gain will not be allowed without written permission.

Trafton Webb Fleetwood, Jr.

ABRUPT ENLARGEMENTS IN SMOOTH AND ROUGH PIPES

A THESIS

Presented to

the Faculty of the Graduate Division

Georgia Institute of Technology

In Partial Fulfillment

of the Requirements for the Degree

Master of Science in Civil Engineering

By

Trafton Webb Fleetwood, Jr.

June 1955

ABRUPT ENLARGEMENTS IN

SMOOTH AND ROUGH PIPES

Approved:

Date Approved by Chairman: May 25, 1955

ACKNOWLEDGMENTS

The writer is grateful to Professor C. E. Kindsvater for his guidance and assistance as thesis director; to Professors M. R. Carstens and David B. Comer for their service as members of the reading committee; to Mr. Homer J. Bates, laboratory technician; and to Mr. R. W. Carter, Hydraulic Engineer, and the U. S. Geological Survey, for their material assistance in making this work possible.

TABLE OF CONTENTS

Page

LIST OF TABLES

LIST OF FIGURES

Figure Page

ABSTRACT

The flow of a fluid through an abrupt area enlargement in a pipe is accompanied by separation, extreme velocity gradients, high internal shear stresses, and exceptional turbulence. The disturbed flow persists over a considerable length of the larger pipe before the motion pattern is restored to its normal, uniform-flow state. Within this reach much of the energy of the entering stream is converted into irrecoverable heat energy. The total amount of energy "lost" in this manner is comprised of two parts: that due to boundary resistance and that due to the excess turbulence in the wake downstream from the enlargement. It was the purpose of this investigation to evaluate the loss of energy due to abrupt enlargements. A major objective of the study was the determination of the relative influence of boundary roughness.

The larger of the two energy (head) losses in the region of flow establishment downstream from an abrupt enlargement is (H_x), which is that part ascribed to the excess turbulence in the wake. This loss depends primarily on the boundary geometry, which, for uniform circular pipes, is adequately expressed by the area-enlargement ratio, A_2/A_1. It can be evaluated from the classic Borda-Carnot equation. The boundary resistance loss (H_f') depends on the enlargement ratio, the Reynolds number of the flow, the relative roughness of the pipe, flow conditions at the entrance, and the distance (L_2) over which the total head loss is measured. This loss can be evaluated from a form of the Darcy-Weisbach

equation in which (f') is the resistance coefficient. Evaluation of (f') as a function of the variables listed depends on experiment.

The experimental part of this investigation was restricted to symmetrical, abrupt enlargements in circular pipes. Tests were made for four enlargement ratios, two degrees of boundary roughness (designated smooth and rough), and a small range of Reynolds numbers in the turbulent range. Entrance characteristics were virtually eliminated as variables by the use of short, smooth nozzles to produce the entering stream.

The conclusions drawn from the experimental program were based primarily on an analysis of the boundary-resistance head loss (H_f') and the resistance coefficient (f') in the first 25 diameters of the larger pipe downstream from the enlargement. This length is believed to be sufficient to contain the larger part of the non-uniform flow.

From the tests made for this investigation, it appears that (f') is influenced only slightly by the Reynolds number but very much by the enlargement ratio and relative roughness. The influence of the enlargement ratio was much greater for the smooth pipe than for the rough pipe. In fact, (f') for the smooth pipe exceeded that for the rough pipe for all values of the enlargement ratio (A_2/A_1) above seven.

For both the smooth pipe and the rough pipe, (f') was smaller than the normal resistance factor (f) for uniform flow when (A_2/A_1) was less than about four. For larger values of the enlargement ratio, (f') was larger than (f), the ratio (f'/f) reaching a maximum value of 12 for an enlargement ratio of 17 in the smooth pipe.

From practical considerations, it was concluded that the observed

difference between (f') and (f) was insignificant. This was demonstrated by a graph showing the relative error (in the total head loss, including H_x) due to using (f) instead of (f'). It was shown that the maximum error from this cause was less than the usual error in estimating (f) for uniform flow.

CHAPTER I

INTRODUCTION

Description of the Problem.--The flow of a fluid from one pipe into another pipe through an abrupt area enlargement is accompanied by separation, extreme velocity gradients, high internal shear stresses, and exceptional turbulence. The disturbances resulting from the enlargement persist over a considerable length of the larger pipe before the motion pattern is restored to its normal, uniform-flow state. Within this reach much of the kinetic energy of the entering stream is converted directly into heat by the viscous shear stresses which occur at the surface of discontinuity between the jet and the surrounding fluid. A smaller part of the initial energy is converted into energy of turbulence, but this is eventually dissipated as heat energy during the decay of the excess turbulence. The remainder of the kinetic energy of the entering stream accrues to the total energy of the decelerated flow downstream from the enlargement.

It is apparent that the total energy loss resulting from the flow of fluids through abrupt enlargements consists of two parts: that due to boundary resistance and that due to separation and the occurrence of a turbulent wake downstream from the enlargement. It follows that the total loss, as well as the relative magnitude of the two components, depends on the relative size of the enlargement, the shape and relative roughness of the adjacent pipe sections, and the Reynolds number of the

flow. In addition, it has been shown that the flow pattern in the enlargement is especially influenced by the velocity distribution and turbulence characteristics of the entering stream.

Purpose and Scope of the Investigation.--It was the purpose of this investigation to evaluate the loss of energy due to abrupt enlargements in pipes. Particular emphasis was placed on the separation of the total energy loss into the two components described above. Thus, a major objective of the study was the determination of the relative influence of boundary roughness.

The investigation was restricted to symmetrical, abrupt enlargements in circular pipes. The experimental program included tests on four degrees of enlargement and two degrees of boundary roughness in the larger pipe, which was nominally six inches in diameter for all tests. Entrance characteristics were virtually eliminated as variables by the use of short, smooth nozzles of four different sizes. All tests were made for flows in the turbulent range. A limited number of tests was made to establish the normal boundary resistance characteristics of the test pipes and the velocity distribution in the nozzles. Test data on the abrupt enlargements included rate of flow, complete piezometric profiles, and selected velocity traverses.

Review of Research on Abrupt Enlargements.--The procedure usually recommended for estimating the energy loss due to abrupt enlargements in pipes is based on the classic "Borda-Carnot" or "Borda" equation,

$$H_x = \frac{(V_1 - V_2)^2}{2g} = \left[\frac{A_2}{A_1} - 1\right]^2 \frac{V_2^2}{2g}, \qquad (1)$$

where (H_x) is the loss of head due to the enlargement exclusive of the boundary resistance loss, (V_1) and (V_2) are the average velocities, and (A_1) and (A_2) are the areas of the small pipe and the large pipe, respectively. The derivation of the Borda equation is based on the simultaneous solution of the one-dimensional energy and momentum equations. These equations are applied to a reach extending from the abrupt enlargement to a section of essentially uniform flow downstream from the enlargement. In both the energy and the momentum equations the influence of boundary resistance is ignored. Thus, for the estimation of the total energy loss in a pipe line which includes an abrupt enlargement, the loss represented by equation 1 is ordinarily added to the computed boundary resistance loss based on the assumption of uniform flow in the pipes adjacent to the enlargement.

One of the first to attempt to substantiate the traditional application of the Borda equation was A. H. Gibson (1)(2). Gibson made tests on small, smooth pipes, covering area ratios (A_2/A_1 = ratio of downstream pipe area to upstream pipe area) from 2.25 to 10.96. He did not take into account the influence of upstream flow conditions, Reynolds number, or relative roughness. He concluded from his tests that the energy loss "increases slightly with the ratio of enlargement and, in pipes with the same ratio of enlargement, is greater the smaller the pipe." A formula proposed by Gibson, based on his experiments, gives values of (H_x) which are four percent greater at $A_2/A_1 = 10.96$ and 5 percent less at $A_2/A_1 = 2.25$ than the values given by equation 1.

Another investigation frequently quoted was performed by W. H. Archer (3). The experimental set-up used by Archer was similar to that

used by Gibson. Archer's tests covered values of A_2/A_1 from 1.451 to 9.32. The tests were made with smooth brass pipes. The published data are insufficient to describe the upstream flow conditions or the Reynolds number. Like Gibson, Archer presented a table based on his experiments which showed the "true" enlargement loss as a percentage of equation 1. Values given in this table, expressed as a function of the enlargement ratio and the velocity in the upstream pipe, varied from 75 percent (A_2/A_1 = infinity, V_1 = 80 feet per second) to 122 percent (A_2/A_1 = 1.25, V_1 = 2 feet per second). Thus, Archer apparently contradicts Gibson's conclusions that the enlargement loss increases with the enlargement ratio. The extreme variation with (V_1) shown by Archer was not reported by Gibson. It should be emphasized, also, that the table prepared by Archer involves a considerable extrapolation of his experimental data.

One of the most recent studies was reported by Kalinske (4). In his investigation, Kalinske was primarily concerned with the internal mechanism of the energy transformation. Kalinske's tests covered only one enlargement ratio and two rates of flow. However, the data taken included much information on the growth and decay of the turbulent wake, mean velocity distribution, and energy dissipation. Among his conclusions were:

(1) The maximum total turbulence energy is a small part of the total energy change taking place. For an abrupt enlargement, the maximum ratio of the turbulence energy to the mean kinetic energy was 0.50.

(2) The principal loss of energy occurs at the surface of the high velocity stream as it passes into the larger pipe. This loss is due to the high local shear stresses developed and is represented by a direct conversion of kinetic energy into heat energy. The turbulence produced is a by-product

of the energy conversion process. During its decay, however, turbulence eventually results in an energy loss.

(3) The turbulence created in the enlargement plays an important role in helping to reduce the velocity of the center portion of the stream.

(4) The energy lost in an enlargement is influenced considerably by the distribution of velocity at the inlet.

In none of the reported investigations has the influence of boundary roughness been investigated. The present investigation was suggested by this observation and by the certain problems which arose in connection with an investigation of abrupt enlargements in open channels (5).

CHAPTER II

THEORETICAL CONSIDERATIONS

Abrupt Enlargements in Pipes.--Figure 1(a) is a definitive sketch for an analysis of flow through abrupt enlargements in pipes. If it is assumed that section (1) is immediately upstream from the enlargement and that the flow in this section is both steady and uniform (parallel velocity vectors) the average piezometric head in the section is equal to the piezometric head at the boundary. Furthermore, because the live stream issuing from the small pipe or nozzle persists without appreciable change in energy or momentum into the region immediately downstream from the enlargement, the piezometric head in this region is equal to the piezometric head at section (1).

The distance (L_2) in figure 1 is assumed to be sufficient to allow for the establishment of uniform flow in the larger pipe. Thus, the velocity distribution at section (2) is assumed to be normal for the Reynolds number and relative roughness of the pipe. The velocity distribution at section (1) depends, in addition, on the length and relative roughness of the smaller pipe as well as any characteristics such as turbulence or whirl which are imposed on the entering stream.

Figure 1(b) is a force free-body of the fluid contained between sections (1) and (2). For generality, it is assumed that the body is non-horizontal. Thus, the external forces acting in the direction of motion include the normal forces (F_{p_1} and F_{p_2}) due to the pressure at the end

sections, the tangential force (F_τ) due to boundary shear, and the body force (F_g) due to the weight of the fluid.

The so-called momentum principle in fluid mechanics is particularly applicable to the analysis of flow through abrupt enlargements. According to this principle, as it pertains to the free-body in figure 1(b), the summation of the external forces in the direction of motion is equal to the change of momentum flux between sections (1) and (2), or

$$F_{p_1} - F_{p_2} + F_g - F_\tau = Q\rho(\beta_2 V_2 - \beta_1 V_1), \tag{2}$$

where (Q) is the total discharge, (ρ) is the mass density, (V) is the average axial velocity, and (β) is a coefficient which accounts for the non-uniformity of velocity distribution in a cross-section.

As indicated in figure 1, $F_{p_1} = p_1 A_2$ and $F_{p_2} = p_2 A_2$, or,

$$F_{p_1} - F_{p_2} = (p_1 - p_2)\frac{\pi D_2^2}{4},$$

where (p_1) and (p_2) are the average pressures at sections (1) and (2), respectively, and (A_2) is the area of the large pipe, assumed to be uniform and circular.

The body force (F_g), which is the effective component of the total weight (W) is, from the figure,

$$F_g = W \sin\theta = \gamma L_2 A_2 \frac{z_1 - z_2}{L_2} = \gamma(z_1 - z_2)\frac{\pi D_2^2}{4},$$

where ($z_1 - z_2$) is the difference in elevation over the length (L_2), and (γ) is the specific weight of the fluid.

The boundary shear force is expressed in terms of an average boundary shear stress ($\bar{\tau}_o$) or an average drag coefficient ($\bar{c}_f$) for the length (L_2),

$$F_\tau = \bar{\tau}_o \pi D_2 L_2 = \left[\bar{c}_f \left(\rho \frac{V_2^2}{2}\right)\right] \pi D_2 L_2 .$$

Similarly, the change in momentum flux can be expressed as,

$$A_2 V_2 \rho (\beta_2 V_2 - \beta_1 V_1) = \rho V_2 (\beta_2 V_2 - \beta_1 V_1) \frac{\pi D_2^2}{4} .$$

When all the above substitutions are made in equation 2, and after it is divided by (γ) and simplified,

$$\left[\frac{p_1}{\gamma} + z_1\right] - \left[\frac{p_2}{\gamma} + z_2\right] - 4 \bar{c}_f \left(\frac{L_2}{D_2}\right) \frac{V_2^2}{2g} = \frac{V_2}{g} (\beta_2 V_2 - \beta_1 V_1) .$$

Substituting the symbol (h) for the piezometric head ($p/\gamma + z$) and (f') for the quantity ($4\bar{c}_f$),

$$h_1 - h_2 - f' \frac{L_2}{D_2} \frac{V_2^2}{2g} = \frac{V_2}{g} (\beta_2 V_2 - \beta_1 V_1) . \qquad (3)$$

If (β_1) and (β_2) are taken to be equal to 1.0; if ($V_2^2/2g$) is subtracted from both sides; and if ($V_1^2/2g$) is added to both sides of equation 3, it can be factored to give,

$$\left[\frac{V_1^2}{2g} + h_1\right] - \left[\frac{V_2^2}{2g} + h_2\right] - f' \frac{L_2}{D_2} \frac{V_2^2}{2g} = \frac{(V_1 - V_2)^2}{2g} . \qquad (4)$$

The right-hand term in equation 4 is the Borda equation for the head loss due to enlargement (equation 1), which is usually derived without any consideration of boundary resistance. The first two quantities in brackets,

on the other hand, represent the total energy heads at sections (1) and (2), respectively. It follows that the third quantity can be described as the total head loss due to boundary resistance in the reach of length (L_2). Letting (H_x) represent the enlargement loss and (H_f') the boundary resistance loss,

$$H_1 - H_2 = H_L = H_f' + H_x, \tag{5}$$

where (H_L) is the total energy loss between sections (1) and (2).

The combination of equations 4 and 5 with the equation of continuity yields,

$$H_L = \left[f' \frac{L_2}{D_2} + \left(\frac{A_2}{A_1} - 1 \right)^2 \right] \frac{V_2^2}{2g} . \tag{6}$$

It is also apparent that (H_f') in equation 5 is similar to the quantity (H_f) given by the Darcy-Weisbach equation for the resistance loss due to uniform flow in pipes,

$$H_f = f \frac{L}{D} \frac{V^2}{2g} . \tag{7}$$

It follows that (f') is similar to (f).

The Influence of Velocity Distribution.--In the foregoing analysis, subsequent to equation 3, it was assumed that the momentum flux coefficients, β_1, and β_2, were equal to 1.0. Prerequisite to this assumption, of course, is the assumption that the velocities at all points in each cross-section are equal; that is, that the velocities are uniformly distributed in the section. It is important that the error due to this assumption be evaluated.

From equation 3, the error in evaluating (H_f') is,

$$\Delta(H_f') = \frac{V_2}{g}\left[(\beta_2 V_2 - \beta_1 V_1) - (V_2 - V_1)\right].$$

Or, simplified and expressed as a dimensionless ratio with respect to $(V_2^2/2g)$,

$$\frac{\Delta(H_f')}{V_2^2/2g} = 2\left[(\beta_2 - 1) - \frac{A_2}{A_1}(\beta_1 - 1)\right]. \tag{8}$$

Similarly, the error in (f') is,

$$\Delta(f') = \frac{2D_2}{L_2}\left[(\beta_2 - 1) - \frac{A_2}{A_1}(\beta_1 - 1)\right], \tag{9}$$

or,

$$\Delta(f') = \frac{D_2}{L_2}\Delta(H_f'). \tag{10}$$

It is apparent that evaluation of the relative errors in (H_f') and (f') due to the assumption of uniform velocity distributions at sections (1) and (2) is dependent on the evaluation of (β_1) and (β_2). The momentum flux coefficients are defined by the relationship,

$$\beta(Q\rho V) = \int^{Q} v\, DQ = \rho \int^{A} v^2\, dA, \tag{11}$$

in which (v) is the velocity at the point represented by the differential area (dA). From equation 11,

$$\beta = \frac{1}{QV}\int^{Q} v\, dQ = \frac{1}{AV^2}\int^{A} (v^2)\, dA. \tag{12}$$

The experimental evaluation of (β) is best accomplished by means of the approximate equation,

$$\beta = \frac{1}{AV^2} \sum^{A} (\bar{v}^2)\ \Delta A, \tag{13}$$

where summation is substituted for integration, and ($\bar{v}$) is the measured average velocity in a small but finite portion of the total area, ΔA.

Beta should not be confused with the coefficient (α, alpha), which is a measure of the error involved in the assumption that the average velocity-head in a cross-section is ($V^2/2g$). Alpha is defined by the equation,

$$\alpha = \frac{1}{QV^2} \int^{Q} (v^2)dQ = \frac{1}{AV^3} \int^{A} (v^3)\ dA, \tag{14}$$

or,

$$\alpha = \frac{1}{AV^3} \sum^{A} (\bar{v})^3\ \Delta A. \tag{15}$$

CHAPTER III

LABORATORY SET-UP

General.--The laboratory tests for this investigation were made in the Hydraulics Laboratory, School of Civil Engineering, Georgia Institute of Technology. The general arrangement of the laboratory equipment is shown on figures 2 and 3.

The principal equipment, including the approach section and the test section, was located in an existing three-foot wide by three-foot deep flume shown in figure 3. This arrangement provided for submergence of the downstream end of the test pipe and the diversion of the discharge into a weighing tank located under the balcony which supported the flume.

Water was supplied from the laboratory's constant-head recirculating system. The approach section consisted of an eight-foot length of twelve-inch pipe equipped with straightening vanes and baffles. A valve in the six-inch pipe line upstream from the approach section was used to regulate the discharge. The maximum discharge used in the test was 1.7 cubic feet per second.

Test Pipes.--The two pipes used for the larger or downstream section of the test section were both built of one-eighth-inch transparent plastic (Lucite or Plexiglas). Both pipes were nominally six inches in outside diameter and were fabricated in short lengths joined by bolt-connected plastic flanges. The lengths and average inside diameters are shown in figure 2.

The test pipes are described in this report as "smooth" and "rough." Each length of smooth pipe was fabricated from two sheets of plastic, butt-joined to form smooth longitudinal seams. End flanges were lathe-turned and fitted to the ends of the pipe sections. Although great care was taken in the fabrication of this pipe, slight irregularities in the inside diameter and mis-matching at the flanged joints prevented it from having the characteristics of hydraulically smooth pipe. An unfortunate, temporary shortage of commercial molded plastic pipe accounted for the local fabrication of the smooth pipe.

The rough pipe used in the tests was made from molded Lucite tubing. To facilitate the application of a sand-grain roughness to the inside surface the pipe sections were cut and re-joined with flanged longitudinal joints. The sand used was a graded river sand which passed a No. 12 U. S. Standard screen sieve and was retained on a No. 14 Tyler screen sieve. The average diameter of the sand was estimated to be 0.005 feet. The sand was cemented to the pipe by means of a full coat of spar varnish. Figure 4 shows the upstream end of the rough pipe section and the rounded-entrance section used for boundary resistance tests. The large flange shown in the photographs was used to attach the test pipe to the twelve-inch approach pipe as shown in figures 2 and 3.

Nozzles.—Velocity non-uniformity and angularity in the flow approaching the test section was largely eliminated by means of the vanes and baffles described above. Transverse variations in velocity in the small pipe were reduced to a minimum by using short (length = 3.0 diameters) smooth nozzles instead of long pipes. Figure 5 shows the four nozzles used for

tests on both the rough and smooth six-inch test pipes. Each nozzle included a rounded entrance and a flange for attachment to the test section. Figure 6 shows one of the nozzles attached to the twelve-inch flange, with the six-inch smooth pipe attached to the downstream side. Details and dimensions of the nozzles as well as the test pipes are shown on figure 7.

Piezometric Profile Measurements.--Piezometric heads were measured by means of piezometers or static tubes connected to a precision manometer. Piezometers for the measurement of static head in section (1) were located in the nozzles a short distance upstream from the enlargement. Their locations are shown on figures 6 and 7. Piezometric-head measurements in the six-inch test sections were made by means of a portable static tube which was inserted through tapped holes along the length of the pipe. The static tube is shown on figure 8. Plugged holes that provided for the insertion of the static tube are shown on figure 6.

Velocity Measurements.--Velocity measurements in the six-inch test pipes were made with a portable pitot-static tube which was inserted in the holes provided for the static tube. A photograph of the tube is shown on figure 8. A simple stagnation tube with a hypodermic needle tip (No. 18 gauge) was used for velocity measurements at the end of the nozzles. Piezometric differentials for the velocity observations were measured on a precision manometer.

Discharge Measurements.--The volume rate of flow for all abrupt enlargement and boundary resistance tests was measured with the laboratory's weighing-tank equipment. Measurements recorded included weight, time,

and water temperature. Weights, measured with a platform-beam scale, were recorded to the nearest pound. Time intervals were measured to the nearest 0.01 second with an electric stop clock.

CHAPTER IV

EXPERIMENTAL PROCEDURE AND TEST RESULTS

Boundary Resistance Tests.--The uniform-flow resistance characteristics of both the smooth and the rough six-inch pipe sections were determined as a basis for comparison with the abrupt enlargement tests. A total of eight tests was made. The results are shown in table 1 and on figures 24 and 25.

The general set-up for the boundary resistance tests was described in the previous chapter. The lengths and average diameters of the test pipes are shown on figure 2. All tests were made with a smooth, rounded entrance section. The pipes were horizontal and at their discharge ends were submerged to ensure full flow.

The resistance characteristics for each kind of pipe were evaluated on the basis of measured piezometric profiles. Piezometric heads were measured with a single static tube equipped with a packing gland for insertion at several wall openings along the length of the pipe. This procedure was used because (1) it avoids the errors due to the individual characteristics of different tubes, (2) it avoids the errors inherent in wall piezometers which are located near mis-matched flanges or in the midst of protuberances which comprise wall roughness, and (3) it avoids the additional head loss which results when several static tubes are located at fixed positions in the pipe.

The resistance coefficient (f in equation 7) was computed on the

basis of the hydraulic gradients at the downstream end of the test reach. These values, taken from smooth curves drawn through the plotted piezometric data, are included in table 1. It is recognized that truly uniform flow cannot be attained in such short reaches as were involved in these tests. However, work by Shapiro and Smith (6) indicates that the normal value of the resistance coefficient would be very nearly attained at the downstream end of the test reach. It is assumed, therefore, that the values of (f) shown in table 1 correspond to the condition of uniform flow.

As a means of classifying the boundary roughness in a pipe, it is customary to compare measured values of (f) with values derived (7) from tests by Nikuradse on sand-roughened pipes. When this was done with the results shown in table 1, the equivalent roughness of the "rough" pipes was 0.034 feet. This value is supposed to correspond to the diameter of the uniform sand grains used by Nikuradse in his tests. It does not compare well, however, with the mean grain size (0.005 feet) of the sand used in fabricating the rough pipe. It is believed that the disagreement reflects the influence of the flanged joints as well as the difference in sand-grain shape, spacing, and method of cementing.

When the results for the "smooth" pipe were plotted on a graph based on the Nikuradse tests, it was apparent that this pipe was not hydraulically smooth. Furthermore, for the four tests shown in table 1, the equivalent sand-grain roughness varied considerably with the Reynolds number. It is apparent that the character of the roughness in the so-called smooth pipe, doubtless due to the flanges and wall irregularities,

is not analogous to the sand roughness described by Nikuradse's results.

Abrupt Enlargement Tests.--The basic data from the abrupt enlargement tests consisted principally of the piezometric profile data shown in tables 2 and 3 and on figures 9 to 16, inclusive. The test program for each of the two kinds of six-inch pipe included four tests on each of the four different nozzles. The four tests made on each set-up covered a small range of Reynolds numbers in the turbulent range.

For all tests, the piezometric heads at eight different stations in the large pipe were measured as differentials with respect to the piezometric head at the beginning of the enlargement (section 1). In the tables and figures which show the results the piezometric head differences are shown as dimensionless ratios with respect to the velocity head in the downstream pipe.

Each of the piezometric profile diagrams, figures 9 to 16, includes a straight line which represents the slope of the hydraulic grade line for uniform flow at an average Reynolds number corresponding to the enlargement tests shown on the figure. By comparison with the downstream ends of the plotted profiles, this line provides a measure of the degree of uniformity achieved by the disturbed flow downstream from the enlargement.

Table 4 includes a summary of the essential data from the piezometric profile measurements. The piezometric head difference (Δh) in this table was taken from smoothed curves drawn through the profile data. For the rough pipe, (Δh) represents the difference in head between section (1) and the section corresponding to the last piezometer in the pipe. For these tests the last piezometer was located a distance

$L_2 = 25.3\ D_2$ from the beginning of the abrupt enlargement. For comparison, values of (Δh) for the smooth pipe represent the difference in piezometric head between section (1) and a section between the last two piezometers at a distance $L_2 = 25\ D_2$ from the beginning of the enlargement.

Velocity Distribution Measurements.---Pitot-static tube traverses to determine the velocity distribution were made in the nozzles as well as the six-inch pipes for two of the four area ratios involved in the enlargement tests.

Measurements in the large pipes consisted of nine velocity determinations in a single diametric section. The pitot-static tube used for these measurements is shown in figure 8. The results of the measurements are shown as dimensionless velocity diagrams on figures 17 to 20, inclusive. Each curve on these figures is labeled to show the location of the section of measurement and the computed values of alpha (equation 16) and beta (equation 14) at that section. Figure 21 is an alternative representation of the velocity traverses made at the section farthest downstream for each of the four tests. The purpose of this figure is to compare the measured velocity distribution at the downstream end of the test reach with the normal velocity curve based on the equations of Prandtl and von Karman (8).

Figure 22 shows the results of velocity traverses made at the end of two of the four nozzles used in the tests. These measurements were made with a single stagnation tube with a hypodermic needle tip. During the measurements the six-inch pipe was removed and the nozzle jet was allowed to discharge into the atmosphere. Each curve shown on the figure

represents the average of two traverses taken on perpendicular diametric sections.

CHAPTER V

ANALYSIS AND DISCUSSION OF TESTS RESULTS

Energy Losses Due to Abrupt Enlargements.--The principal results of this investigation are shown in table 4 and on figures 23 to 28, inclusive. The computations leading to the summary data contained in table 4 are explained on a page of footnotes accompanying the table. All of the data plotted on the summary figures are shown in the table.

Theoretical considerations in Chapter II lead to the conclusion that the total loss of energy in the region of non-uniformity downstream from an abrupt enlargement is comprised of two parts. The largest of these, usually, is (H_x), the loss resulting from the excess shear stresses which occur in the turbulent wake. This loss is believed to be primarily dependent on boundary geometry--which, in the case of circular pipes, is represented mainly by the enlargement ratio, A_2/A_1. The second loss is (H_f'), which is the accumulated boundary resistance loss in the reach considered. This loss is believed to depend on the enlargement ratio, the Reynolds number, the relative roughness of the pipe, flow conditions at the entrance, and the distance from the beginning of the enlargement.

Approximate analyses performed in Chapter II, ignoring the influence of velocity non-uniformities in both pipes, suggest that (H_x) can be evaluated from the classic Borda equation, equation 1. Thus, the residual loss (H_f') must be evaluated from experiments which embrace all of the independent variables. If upstream flow conditions are eliminated it follows that,

$$H_f' = \phi\left(\underline{R}_2, \frac{k}{D_2}, \frac{A_2}{A_1}, \frac{L_2}{D_2}\right) , \qquad (16)$$

where (ϕ, phi) means "function of," $\underline{R}_2$ is the Reynolds number of the larger pipe, (k/D_2) is the relative roughness of the pipe, (A_2/A_1) is the enlargement ratio, and (L_2/D_2) is the length, relative to the pipe diameter, of the non-uniform flow reach considered in the evaluation of the total head loss (H_L).

If, from practical considerations, (L_2) is defined arbitrarily as a constant length sufficient for the establishment of uniform flow downstream from the enlargement, the variables are reduced to $(\underline{R}_2)$, (k/D_2) and (A_2/A_1). The tests performed for this investigation define (H_f') over a limited range of values of $(\underline{R}_2)$ in the turbulent range, two values of (k/D_2), and four values of (A_2/A_1). For all tests (L_2/D_2) was taken to be approximately 25.

Several reasons can be given for believing that a reach of length $L_2 = 25\ D_2$ is sufficient to contain the major part of the non-uniform flow downstream from the enlargement. Figures 9 to 16, for example, show that the hydraulic grade lines described by the piezometric profiles for the enlargement tests are virtually parallel to the uniform-flow grade line at $L_2/D_2 = 25$. Figure 21, furthermore, shows that the velocity distribution at the downstream end of the test reach is very nearly normal in comparison with the Karman-Prandtl equations. Finally, Kalinske (4) has shown that the turbulence energy in the flow downstream from an abrupt enlargement $(A_2/A_1 = 3)$ was essentially normal after a distance of 17 diameters.

It has been observed that (H_x) is the larger part of the total energy loss in the non-uniform flow reach downstream from an enlargement. This is clearly demonstrated on figure 23, which shows the residual loss, $H_f' = H_L - H_x$, as a percentage of the total measured head loss. It is apparent that (H_f') is a relatively insignificant part of the total loss for values of (A_2/A_1) greater than about 5.0. This conclusion is of considerable importance in evaluating the subsequent conclusions regarding (H_f') at higher values of (A_2/A_1).

The coefficient (f') was described in Chapter II as a boundary resistance coefficient similar to (f) in the Darcy-Weisbach equation for uniform flow in pipes. Values of (f') computed from the test results are shown in table 4 and on figures 24 and 25. From the figures it is apparent that (f') depends only slightly on the Reynolds number but very much on the enlargement ratio. It appears, furthermore, that the influence of the enlargement ratio is greater for the smooth pipe than for the rough pipe. It is also evident, especially for the rough pipe, that (f') is lower than (f) at small enlargement ratios.

Figure 26, which emphasizes the influence of (A_2/A_1) on (f'), is an alternative method of showing the data on figures 24 and 25. Values of R_2, not shown for the plotted points, can be obtained from table 4.

Figure 27 is a dimensionless plot of the data shown on figure 26. From this diagram it is apparent that f' (or H_f') can be as much as 12 times f (or H_f) when $A_2/A_1 = 17$. However, it should be emphasized that, from figure 23, H_f' (not H_f) is only about three percent of the total loss for this condition.

From practical considerations, figure 28 is probably the most significant of the summary diagrams. This figure, based on all the tests for both the smooth and the rough pipes, shows the error in the assumption that $H_f' = H_f$, expressed as a percentage of the total energy loss in the first 25 diameters of the larger pipe. It is significant that the error is small and within the usual limits of accuracy for estimating resistance coefficients for uniform flow. It is also significant that the error, expressed as $(H_f'-H_f)/H_L$, is positive and relatively constant for values of (A_2/A_1) above 5.0, that it is negative for small enlargement ratios, and that it is relatively independent of the Reynolds number in the range investigated.

Influence of Velocity Distribution.—Analyses in the preceding section were based on a summary of test results in which the influence of velocity distribution at sections (1) and (2) was ignored. Equations 8 and 9 provide a measure of the error resulting from this procedure.

According to equation 8 the relative error in computing (H_f') without regard for velocity distribution depends on A_2/A_1, β_1, and β_2. The error in (f') depends, in addition, on the value of (L_2/D_2) used in evaluating (H_f'). It is believed that the results of the velocity distribution tests shown on figures 17 to 22, inclusive, although they do not cover a full range of enlargement ratios, are sufficient to indicate the relative magnitude of the error in values of (H_f') and (f') given in table 4.

For both tests shown on figure 22, (β_1) is 1.002. This value agrees well with values determined by Peters (9) for the entrance to smooth pipes. From figures 17 and 18, (β_2) at $L/D_2 = 28.8$ is 1.007 for

A_2/A_1 = 7.01 and 1.003 for A_2/A_1 = 1.87. For the rough pipes, from figures 19 and 20, (β_2) at L/D_2 = 25.3 is 1.05 for A_2/A_1 = 6.85 and 1.01 for A_2/A_1 = 1.82. When these values are substituted in equations 8 and 9, the maximum error (for A_2/A_1 = 6.85 and the rough pipe) in (H_f'), expressed as a ratio with respect to ($V_2^2/2g$), is $\pm$ 0.072, and the corresponding maximum error in (f') is $\pm$ 0.0028. As these values are within the range of experimental accuracy, it is believed that the influence of velocity distribution, for the test conditions, can be ignored.

CHAPTER VI

CONCLUSIONS

1. The total head loss in a pipe line containing an abrupt enlargement is comprised of two parts. The larger loss is that due to the excess turbulence in the wake of the enlargement, H_x. The second is a boundary resistance loss, H_f'.
2. The loss (H_x) depends primarily on the enlargement ratio. It can be evaluated from the classic Borda-Carnot equation.
3. The boundary resistance loss, H_f', depends on the enlargement ratio, the Reynolds number, the relative roughness of the pipe, flow conditions at the entrance, and the distance (L_2) over which the total head loss is measured. This loss can be evaluated from a form of the Darcy-Weisbach equation in which (f') is the resistance coefficient.
4. From tests covering a small range of Reynolds numbers in the turbulent range and in which entrance conditions and length were constants ($L_2 = 25\ D_2$), it was shown that (f') is influenced only slightly by Reynolds number but very much by the enlargement ratio and relative roughness.
5. The influence of the enlargement ratio is greater for a smooth pipe than for a moderately rough pipe.
6. For both smooth and rough pipes, (f') is slightly smaller than the uniform-flow resistance coefficient (f) at values of the enlargement

(A_2/A_1) less than about four. For higher values of the enlargement ratio, (f') becomes much larger than (f), the ratio (f'/f) reaching a maximum of 12 for an enlargement (area) ratio of 17 in smooth pipe.

7. In comparison with the total head loss downstream from abrupt enlargements, the observed difference between (f') and (f) is insignificant. Thus, the relative error due to using (f) instead of (f') in the region of flow establishment is less than the usual error in estimating (f) for uniform flow.

REFERENCES

(1) Gibson, A. H., "The Conversion of Kinetic Energy in the Flow of Water through Passages Having Divergent Boundaries," Proceedings of the Royal Society of the Arts, Vol. 83, 1910, pp. 366-378.

(2) Gibson, A. H., "On the Resistance to Flow of Water through Pipes or Passages having Divergent Boundaries," Transactions of the Royal Society of Edinburgh, Vol. 48, Part I, No. 5, 1910, pp. 97-116.

(3) Archer, W. H., "Loss of Head due to Enlargement in Pipes," Transactions, A.S.C.E., Vol. 76, 1913, pp. 999-1026.

(4) Kalinske, A. A., "Conversion of Kinetic to Potential Energy in Flow Expansions," Transactions, A.S.C.E., Vol. 111, 1946, pp. 355-390.

(5) Tracy, H. J., and Carter, R. W., "Backwater Effects of Open Channel Constrictions," Proceedings Separate No. 413, A.S.C.E., Vol. 80, February 1954.

(6) Shapiro, A. H., and Smith, R. D., "Friction Coefficients in the Inlet Length of Smooth Round Tubes," Technical Note No. 1785, 1948, National Advisory Committee for Aeronautics.

(7) Rouse, Hunter, Elementary Mechanics of Fluids, John Wiley and Sons, 1946, p. 211.

(8) Ibid., p. 198.

(9) Peters, H., "Conversion of Energy in Cross-Sectional Divergences under Different Conditions of Inflow," Translation, Technical Memorandum No. 737, 1934, National Advisory Committee for Aeronautics.

APPENDIX

Table 1. Summary of Boundary Resistance Tests

Test	R_2	h_f/L (1)	f (2)
13S	4.37×10^5	0.0469	0.0163
14S	2.46×10^5	.0175	0.0190
15S	1.03×10^5	.0356	0.0220
16S	3.33×10^5	0.0298	0.0175
13R	4.78×10^5	0.1223	0.0592
14R	3.09×10^5	0.0523	0.0607
15R	1.59×10^5	0.0135	0.0594
16R	2.88×10^5	0.0572	0.0599

(1) Slope of piezometric line at downstream end of test reach.

(2) Resistance coefficient in the Darcy-Weisbach equation.

Table 2. Piezometric Profiles, Smooth Pipe

Test No.	$\frac{A_2}{A_1}$	R_2	$(h-h_1) \div V_2^2/2g$ Distance, L/D_2							
			0.87	1.73	2.95	3.82	8.00	16.3	20.4	28.8
1S	7.01	1.57×10^5	- 4.48	-0.366	4.33	6.67	10.4	10.3	10.2	10.1
2S	7.01	9.55×10^4	- 0.788	-0.189	5.31	8.62	10.3	10.2	10.0	9.83
3S	7.01	2.82×10^4	- 0.534	1.78	6.94	9.43	10.7	10.3	9.96	9.79
4S	17.6	6.04×10^4	-12.0	-18.2	5.69	21.4	21.8	25.1	24.6	24.3
5S	17.6	2.89×10^4	-10.1	-12.4	9.90	22.2	23.8	24.8	24.2	23.6
6S	17.6	1.75×10^4	- 9.17	-12.8	11.9	20.2	22.9	23.4	23.4	23.4
7S	3.43	2.85×10^5	- 0.824	1.83	3.19	4.04	4.58	4.50	4.40	4.28
8S	3.43	1.95×10^5	- 0.026	1.77	3.19	4.04	4.53	4.43	4.35	4.23
9S	3.43	1.15×10^5	- 0.225	1.69	3.11	3.98	4.54	4.39	4.28	4.12
10S	1.87	4.00×10^5	0.400	1.39	1.52	1.55	1.56	1.47	1.39	1.25
11S	1.87	2.52×10^5	0.358	1.37	1.52	1.54	1.56	1.43	1.36	1.21
12S	1.87	1.26×10^5	0.336	1.37	1.53	1.56	1.55	1.42	1.30	1.13

$(h-h_1)$ = Piezometric head difference referred to Section 1 at the abrupt enlargement.

L/D_2 = Distance from abrupt enlargement referred to diameter of larger pipe.

Table 3. Piezometric Profiles, Rough Pipe

Test No.	$\frac{A_2}{A_1}$	R_2	$(h-h_1) \div V_2^2/2g$ Distance, L/D_2							
			1.06	2.11	3.16	4.22	8.44	14.0	21.1	25.3
1R	17.1	6.81×10^4	-11.8	-8.82	16.4	27.7	30.2	29.9	29.6	29.4
2R	17.1	5.19×10^4	-14.3	-9.43	17.8	31.1	34.3	33.6	29.6	29.3
3R	17.1	2.79×10^4	-17.5	-6.83	19.4	28.0	30.4	30.1	29.7	29.3
4R	6.85	1.59×10^5	- 1.10	1.13	6.49	9.75	10.7	10.5	10.1	9.89
5R	6.85	8.93×10^4	- 1.93	0.774	6.19	9.68	10.7	10.4	10.2	9.81
6R	6.85	3.90×10^4	- 3.66	0.495	5.25	9.41	10.3	10.0	9.60	9.31
7R	3.34	3.04×10^5	0.010	2.34	3.39	3.99	4.20	3.88	3.51	3.32
8R	3.34	1.77×10^5	-0.069	2.25	3.22	3.94	4.16	3.86	3.48	3.30
9R	3.34	9.79×10^4	-0.0749	2.11	3.35	4.00	4.10	3.79	3.41	3.20
10R	1.82	3.44×10^5	0.755	1.31	1.32	1.29	1.13	0.830	0.456	0.249
11R	1.82	2.34×10^5	0.745	1.31	1.33	1.29	1.11	0.817	0.457	0.245
12R	1.82	1.45×10^5	0.713	1.30	1.34	1.29	1.10	0.822	0.420	0.229

$(h-h_1)$ = Piezometric head difference referred to Section 1 at the abrupt enlargement.

L/D_2 = Distance from abrupt enlargement referred to diameter of larger pipe.

Table 4. Summary of Tests on Abrupt Enlargements

Test No.	$\frac{A_2}{A_1}$	Q	$\frac{R_2}{10^4}$	$\frac{V_1^2}{2g}$	$\frac{V_2^2}{2g}$	Δh	H_L	H_2	H_x	H_2'	$\frac{H_f'}{H_L}$ (Pct.)	$\frac{H_f'-H_f}{H_L}$ (Pct.)	f'	f	$\frac{f'}{f}$
(1)	(2)	(3)	(4)	(5)	(6)	(7)	(8)	(9)	(10)	(11)	(12)	(13)	(14)	(15)	(16)
1S	7.01	0.621	15.7	9.060	0.183	1.864	7.020	0.0900	6.660	0.360	5.3	3.80	0.078	0.0204	3.80
2S	7.01	0.365	9.55	3.130	0.0634	0.634	2.430	0.0361	2.310	0.123	5.0	3.50	0.078	0.0223	3.50
3S	7.01	0.109	2.82	0.279	0.00562	0.056	0.217	0.0041	0.206	0.0110	5.1	3.20	0.078	0.0301	2.60
4S	17.6	0.232	6.04	7.860	0.0255	0.627	7.210	0.0156	6.980	0.230	3.2	3.00	0.36	0.0249	14.4
5S	17.6	0.112	2.89	1.840	0.00596	0.143	1.690	0.0043	1.640	0.050	3.0	2.70	0.34	0.0300	11.3
6S	17.6	0.0678	1.75	0.673	0.00218	0.051	0.620	0.00180	0.598	0.022	3.5	3.30	0.40	0.0339	11.8
7S	3.43	1.123	28.5	7.050	0.598	2.594	3.860	0.269	3.540	0.320	8.3	1.3	0.021	0.0183	1.10
8S	3.43	0.754	19.5	3.180	0.270	1.160	1.750	0.130	1.600	0.150	8.6	1.1	0.022	0.0196	1.10
9S	3.43	0.454	11.5	1.150	0.0977	0.411	0.641	0.0525	0.579	0.062	9.7	1.0	0.025	0.0216	1.20
10S	1.87	1.567	40.0	4.080	1.160	1.541	1.370	0.495	0.885	0.485	35.4	-0.73	0.017	0.0172	0.99
11S	1.87	0.986	25.2	1.610	0.461	0.591	0.558	0.213	0.350	0.208	37.3	-0.90	0.018	0.0187	0.96
12S	1.87	0.489	12.6	0.397	0.113	0.133	0.146	0.0595	0.0862	0.060	41.0	0.68	0.022	0.0217	1.01
1R	17.1	0.218	6.81	6.960	0.0238	0.699	6.240	0.036	6.170	0.070	1.1	0.54	0.11	0.0600	1.83
2R	17.1	0.167	5.19	4.080	0.0140	0.410	3.660	0.021	3.620	0.040	1.1	0.52	0.11	0.0600	1.83
3R	17.1	0.104	2.79	1.580	0.00542	0.159	1.420	0.008	1.400	0.020	1.4	0.85	0.12	0.0600	2.00
4R	6.85	0.577	15.9	7.830	0.167	1.652	6.010	0.251	5.710	0.300	5.0	0.82	0.071	0.0600	1.18
5R	6.85	0.325	8.93	2.480	0.0530	0.520	1.910	0.079	1.810	0.100	5.2	1.0	0.073	0.0600	1.22
6R	6.85	0.142	3.90	0.474	0.0101	0.096	0.368	0.015	0.346	0.022	6.0	1.9	0.086	0.0600	1.43
7R	3.34	1.092	30.4	6.670	0.598	1.987	4.090	0.901	3.270	0.820	20.0	-2.2	0.053	0.0600	0.88
8R	3.34	0.636	17.7	2.260	0.203	0.670	1.390	0.306	1.110	0.280	20.1	-2.0	0.054	0.0600	0.90
9R	3.34	0.365	9.79	0.745	0.0668	0.215	0.463	0.101	0.367	0.096	20.8	-1.1	0.057	0.0600	0.95
10R	1.82	1.362	34.4	3.080	0.930	0.232	1.920	1.402	0.625	1.300	67.4	-5.4	0.055	0.0600	0.92
11R	1.82	0.911	23.4	1.330	0.416	0.102	0.862	0.627	0.280	0.582	67.5	-5.2	0.055	0.0600	0.92
12R	1.82	0.560	14.5	0.521	0.157	0.036	0.328	0.237	0.106	0.222	67.7	-4.6	0.056	0.0600	0.93

*See footnotes on following page for explanation of column headings.

Footnotes to Table 4

Col. 2 - The same four nozzles were used and therefore A_1 was constant for all tests; however, (D_2) for the smooth pipe was 0.480 feet, whereas (D_2) for the rough pipe was 0.474 feet.

Col. 3 - Measured discharge in cubic feet per second.

Cols. 5 and 6 - Velocity heads were computed on the basis of average velocities; i.e., velocity was assumed to be uniformly distributed.

Col. 7 - $\Delta h = h_2 - h_1$ is the measured difference in piezometric head between the abrupt enlargement ($L/D_2 = 0$) and the piezometric section at $L/D_2 = 25.0$ (smooth pipe) or $L/D_2 = 25.3$ (rough pipe).

Col. 8 - $H_L = V_1^2/2g - \Delta h - V_2^2/2g$ = total energy loss in the first 25 (or 25.3) diameters of the larger pipe.

Col. 9 - $H_f = f(L/D_2)\ V_2^2/2g$ = computed friction loss, assuming uniform flow downstream from the abrupt enlargement. Values of (f) taken from Fig. 24 or Fig. 25 for $A_2/A_1 = 1.0$.

Col. 10 - $H_x = (V_1 - V_2)^2/2g$ = head loss due to abrupt enlargement, according to the Borda equation.

Col. 11 - $H_f' = H_L - H_x$ = residual head loss attributed to boundary resistance in the 25-diameter reach downstream from the enlargement.

Col. 14 - (f') is the resistance coefficient in the Darcy-Weisbach equation based on (H_f') as defined above.

Col. 15 - Values of (f) taken from Fig. 24 or Fig. 25 for $A_2/A_1 = 1.0$ and for values of R_2 in Col. 4.

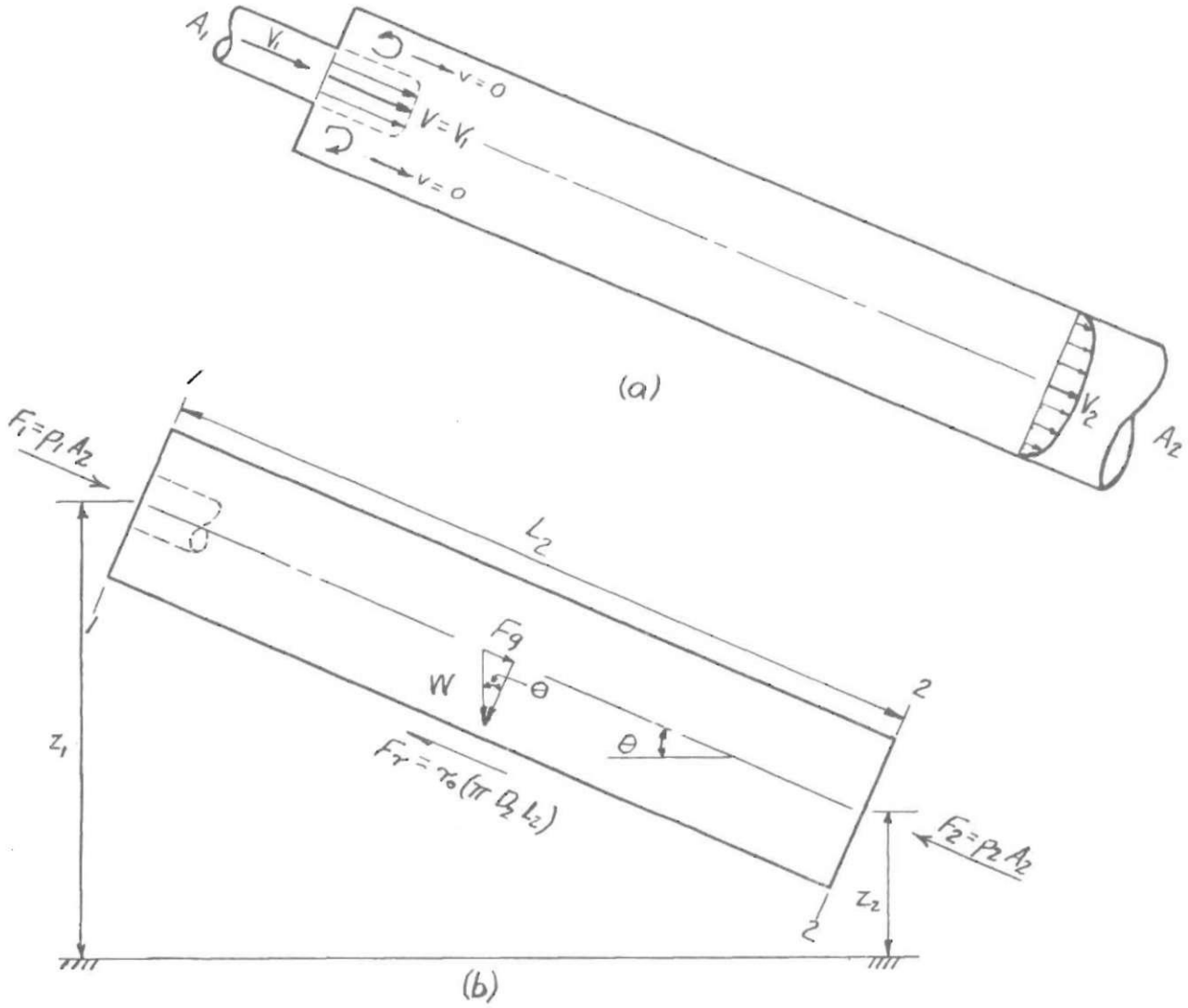

Fig. 1. Definition Sketch of Flow in an Abrupt Enlargement.

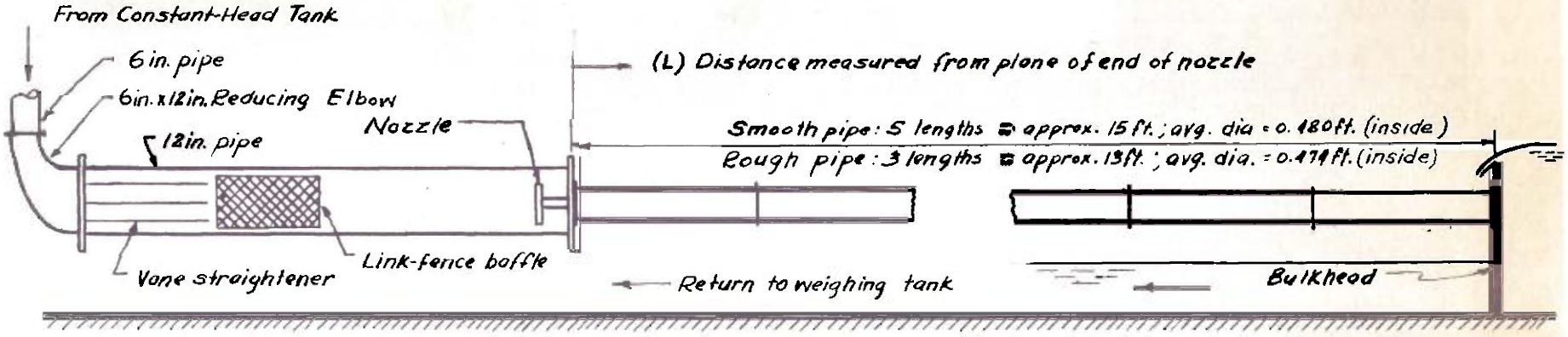

Fig. 2. Laboratory Set-Up

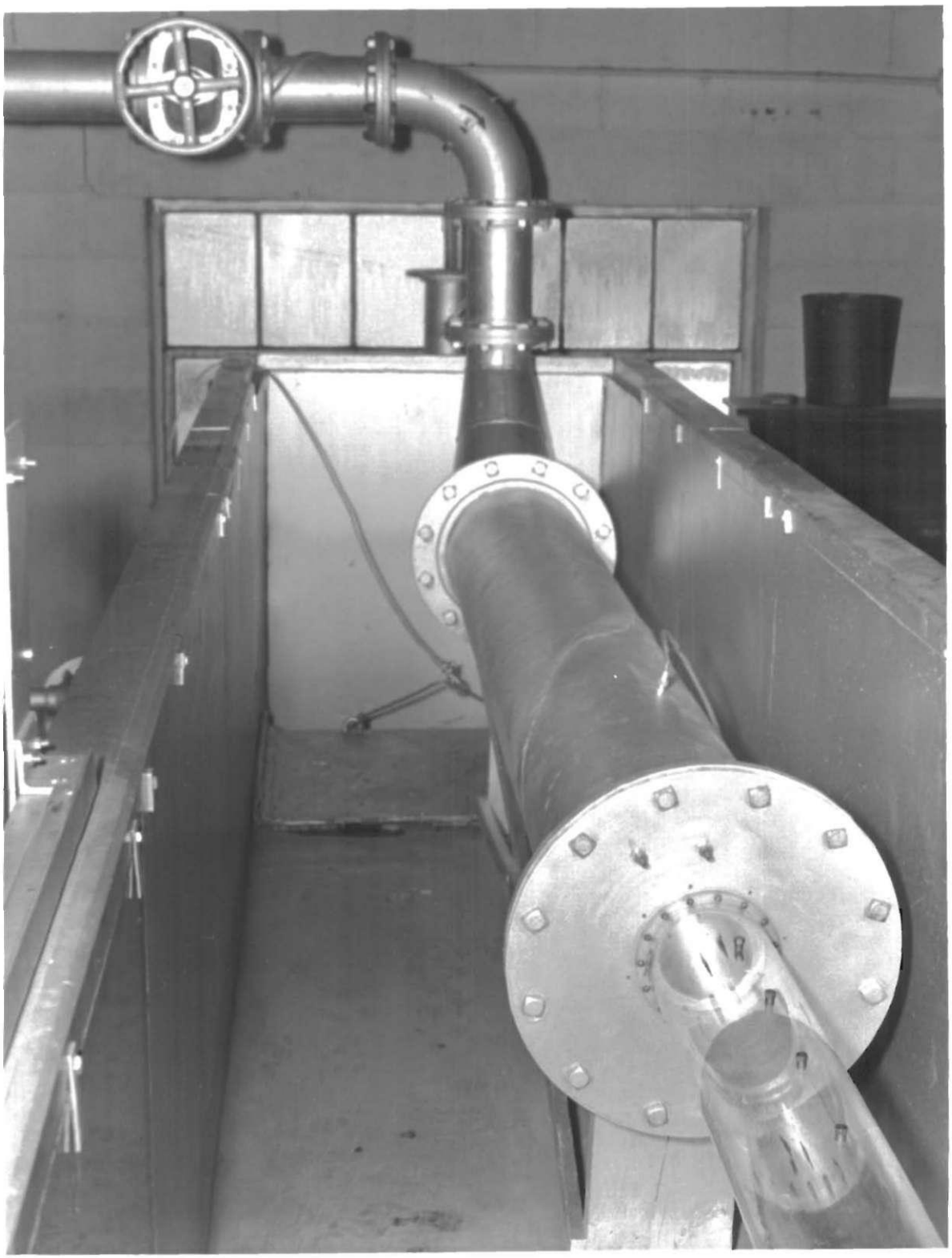

FIGURE 3. UPSTREAM END OF TEST SECTION.

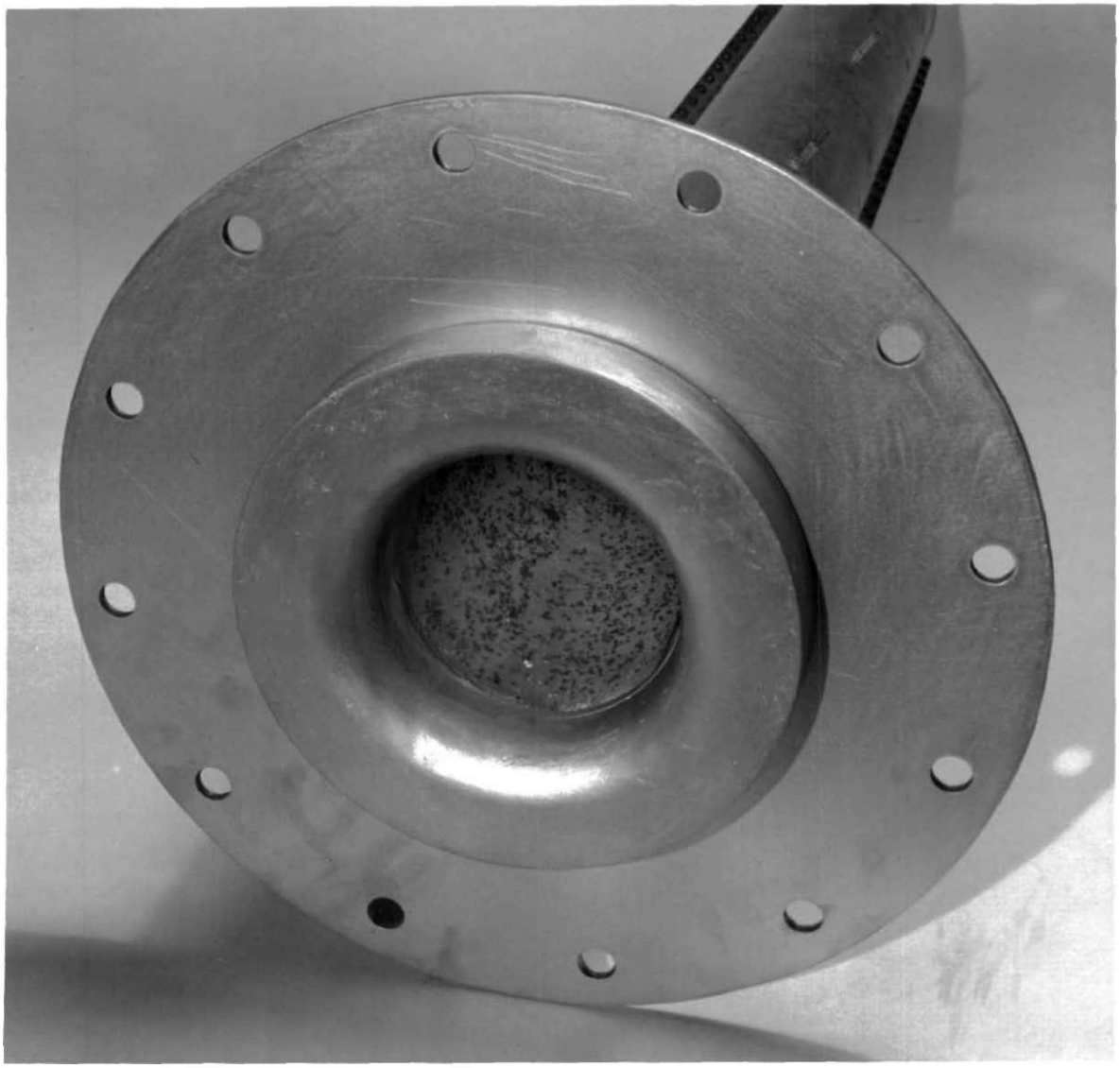

FIGURE 4. ENTRANCE FOR BOUNDARY RESISTANCE TESTS (ROUGH PIPE).

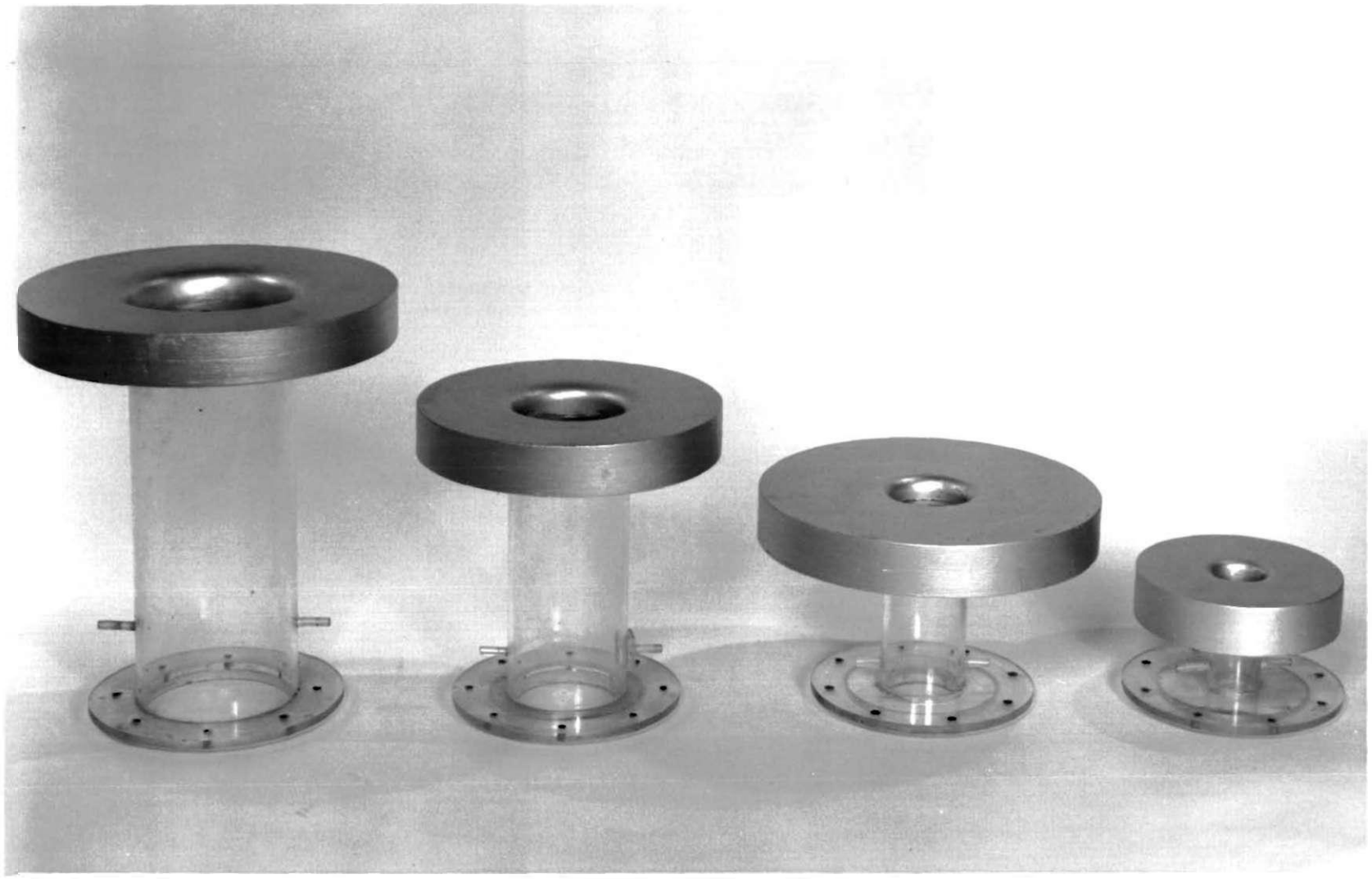

FIGURE 5. NOZZLES USED FOR ALL TESTS.

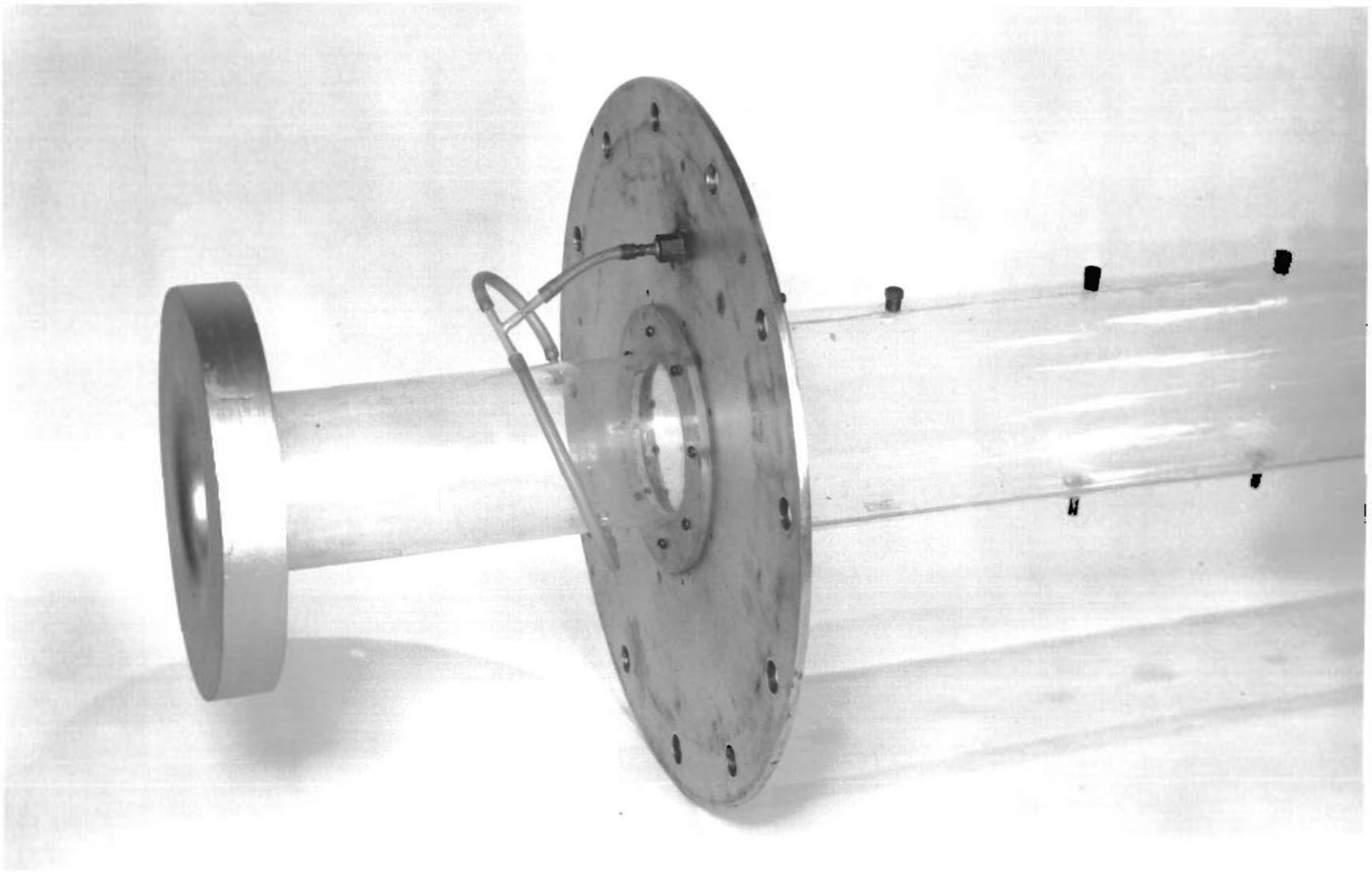

FIGURE 6. PIPE-NOZZLE ASSEMBLY (A_2/A_1 = 1.87).

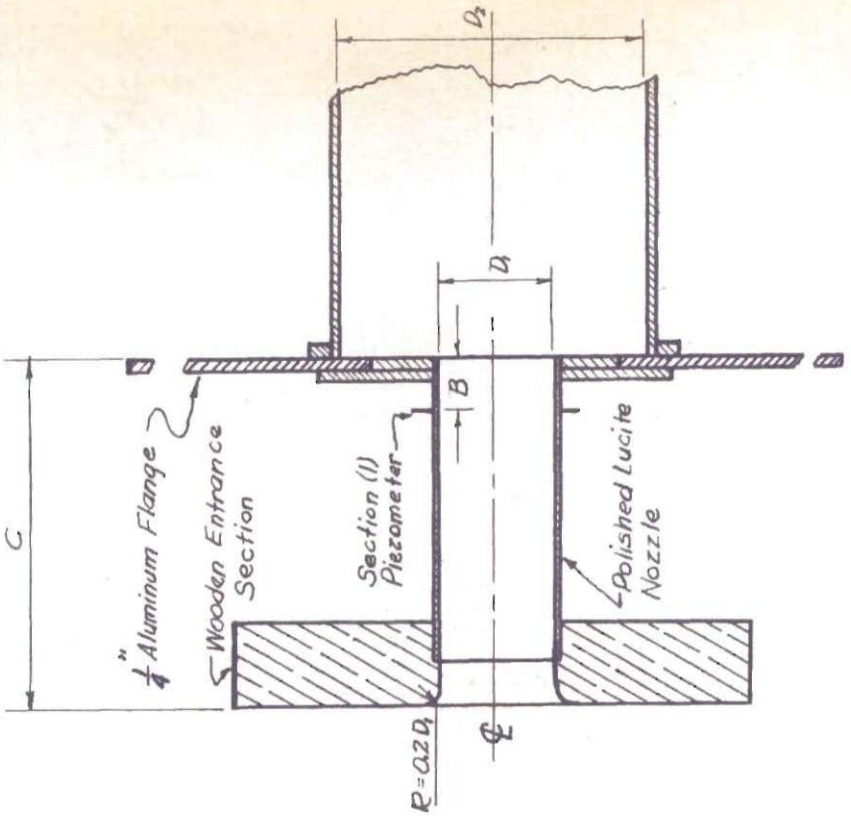

Details of Nozzle and Pipe

D_1	D_2 Smooth	D_2 Rough	A_2/A_1 Smooth	A_2/A_1 Rough	B	C
Ft.	Ft.	Ft.			Ft.	Ft.
0.115	0.480	0.474	1.87	1.82	0.0833	0.345
0.181	0.480	0.474	3.45	3.34	0.0833	0.542
0.259	0.480	0.474	7.01	6.85	0.125	0.775
0.351	0.480	0.474	17.6	17.1	0.217	1.052

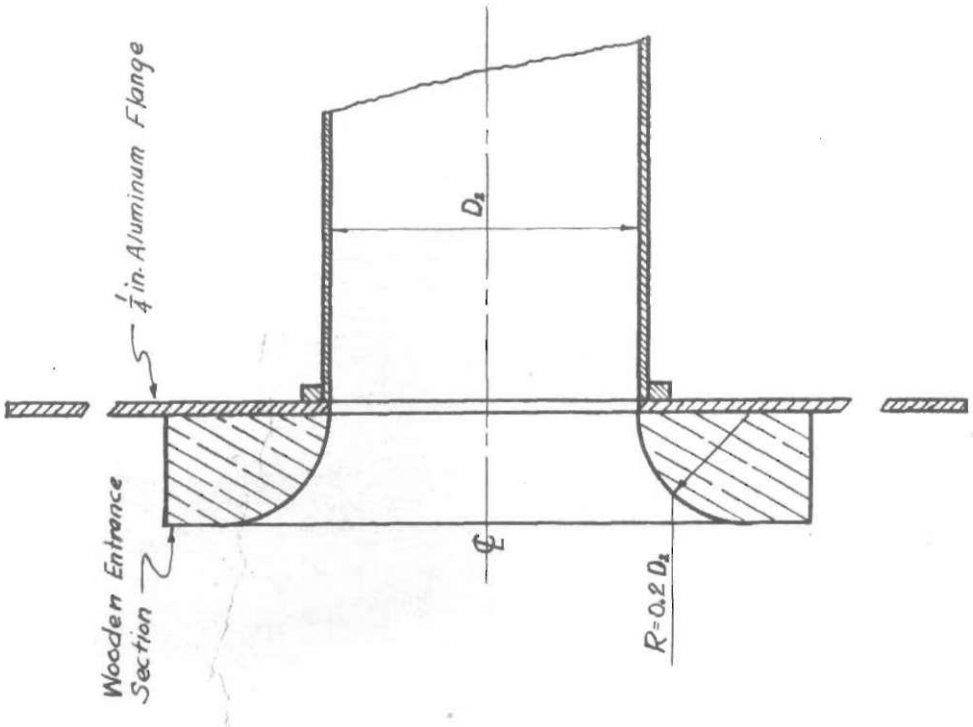

Details of Pipe Entrance for Friction Tests

Fig, 7. Details of Nozzles and Pipe Entrance Sections

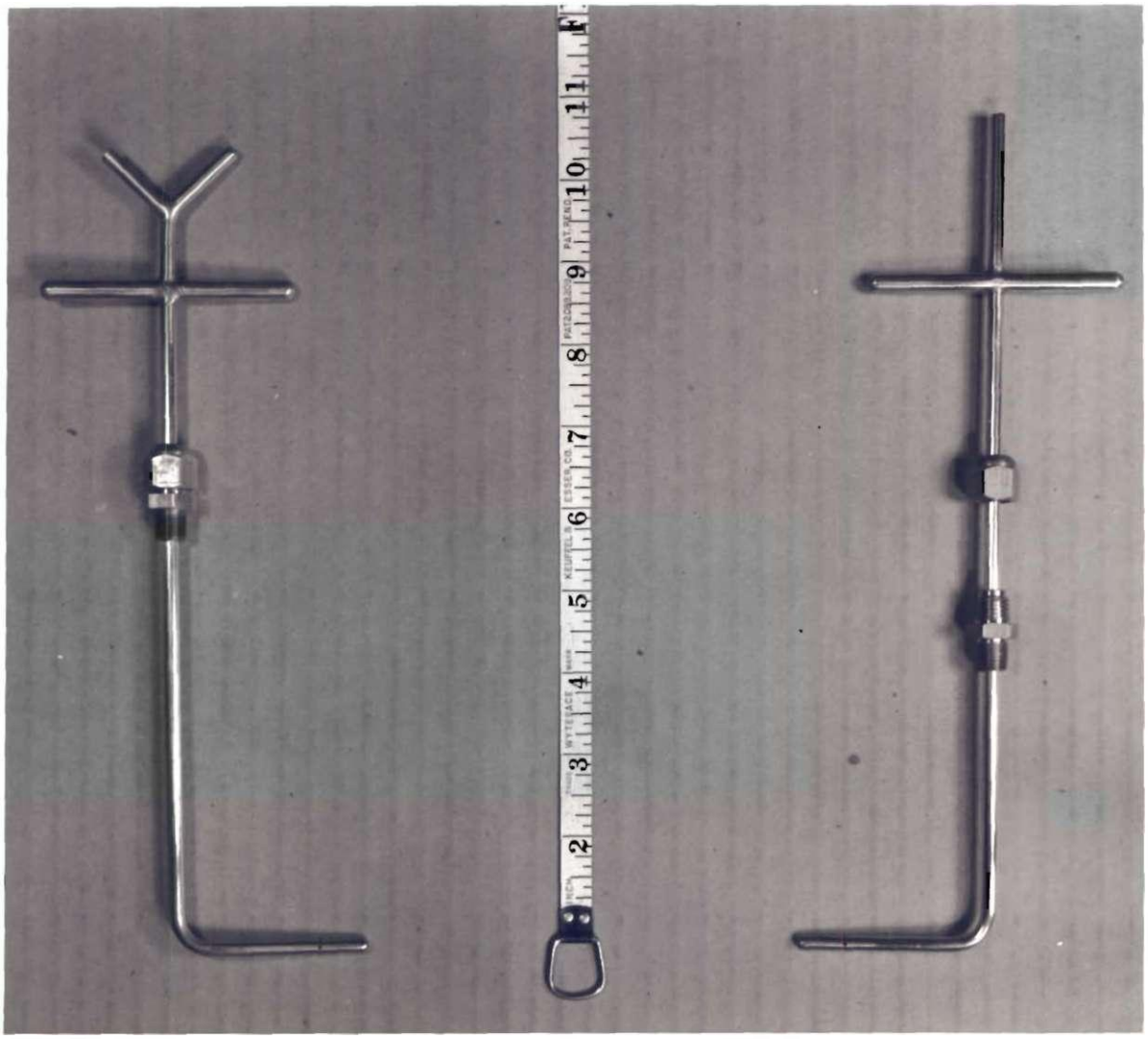

(Left) Pitot-Static Tube
(Right) Static Tube

FIGURE 8. INSTRUMENTS USED FOR VELOCITY AND PRESSURE MEASUREMENTS.

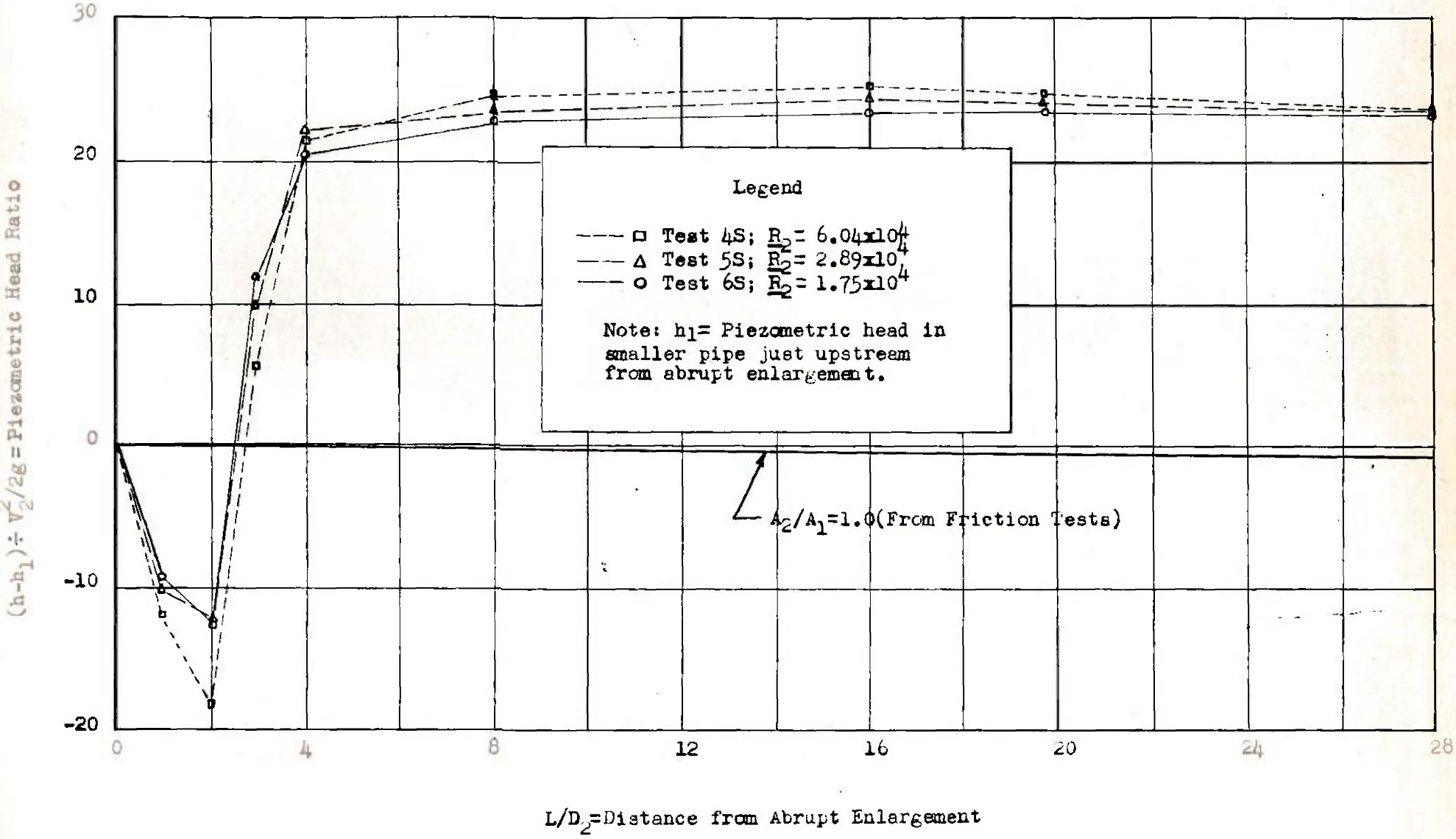

Fig. 9. Piezometric Profiles, Smooth Pipe, $A_2/A_1 = 17.6$

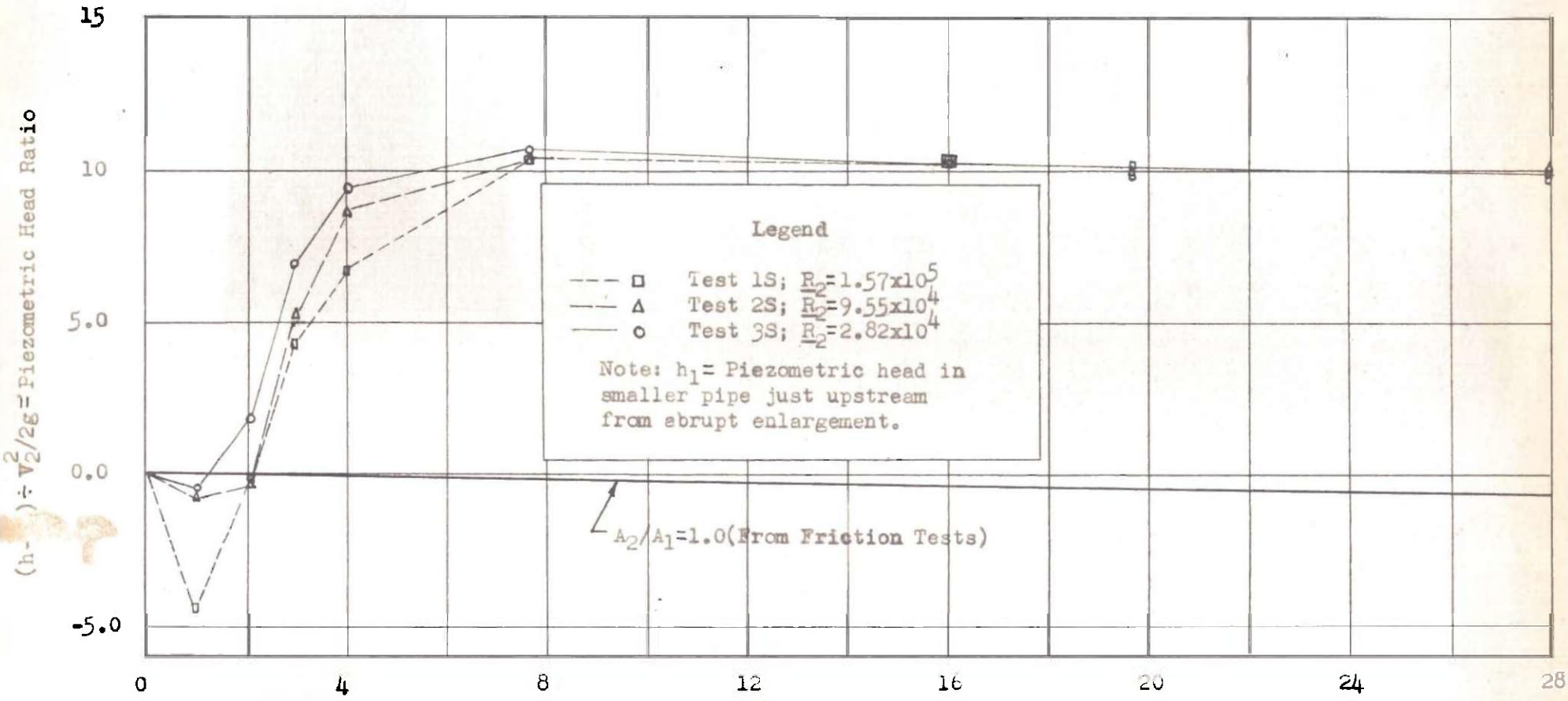

Fig.10. Piezometric Profiles, Smooth Pipe, A_2/A_1= 7.01

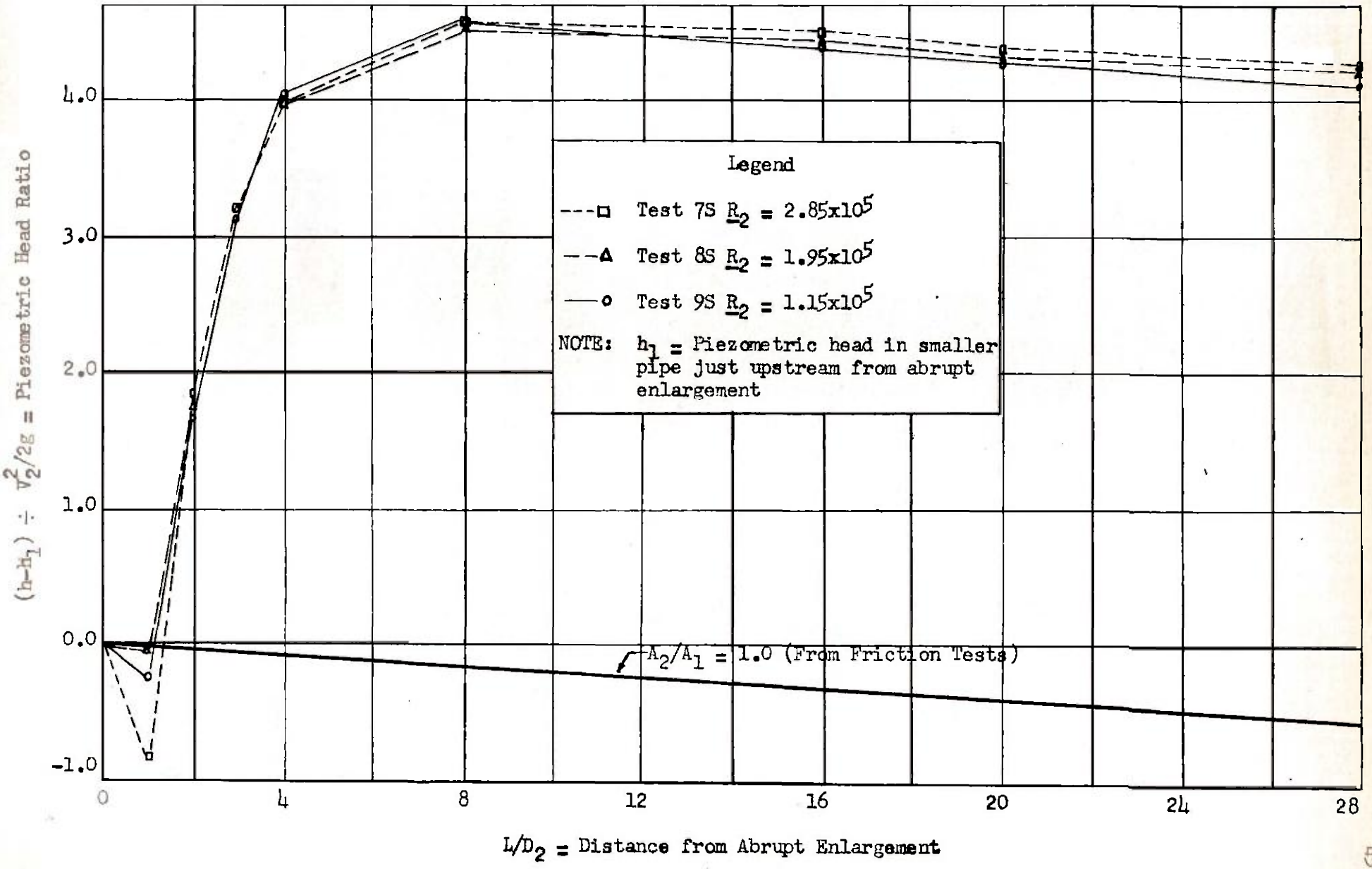

Fig. 11. Piezometric Profiles, Smooth Pipe, A_2/A_1 = 3.43

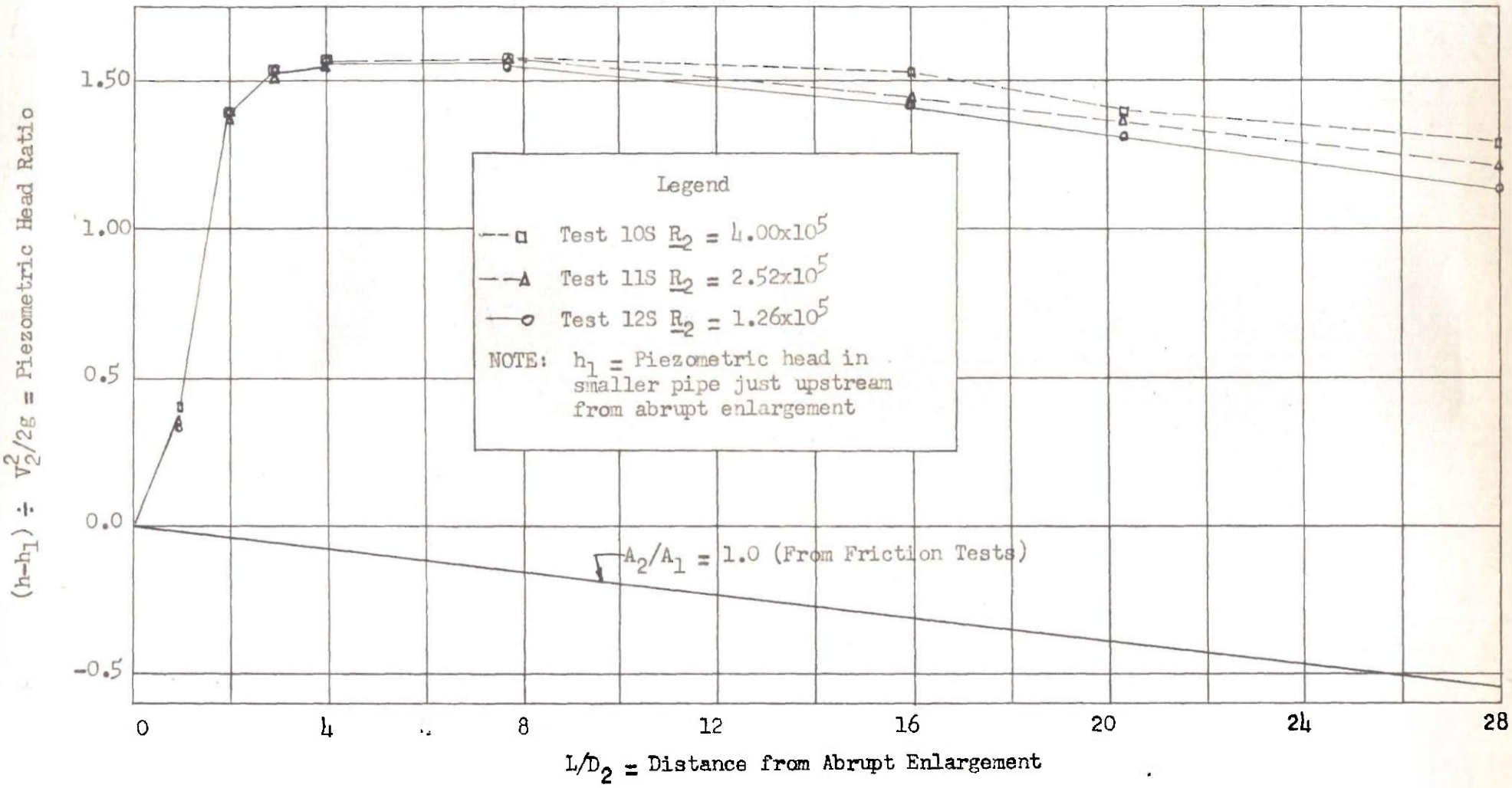

Fig. 12. Piezometric Profiles, Smooth Pipe, $A_2/A_1 = 1.87$

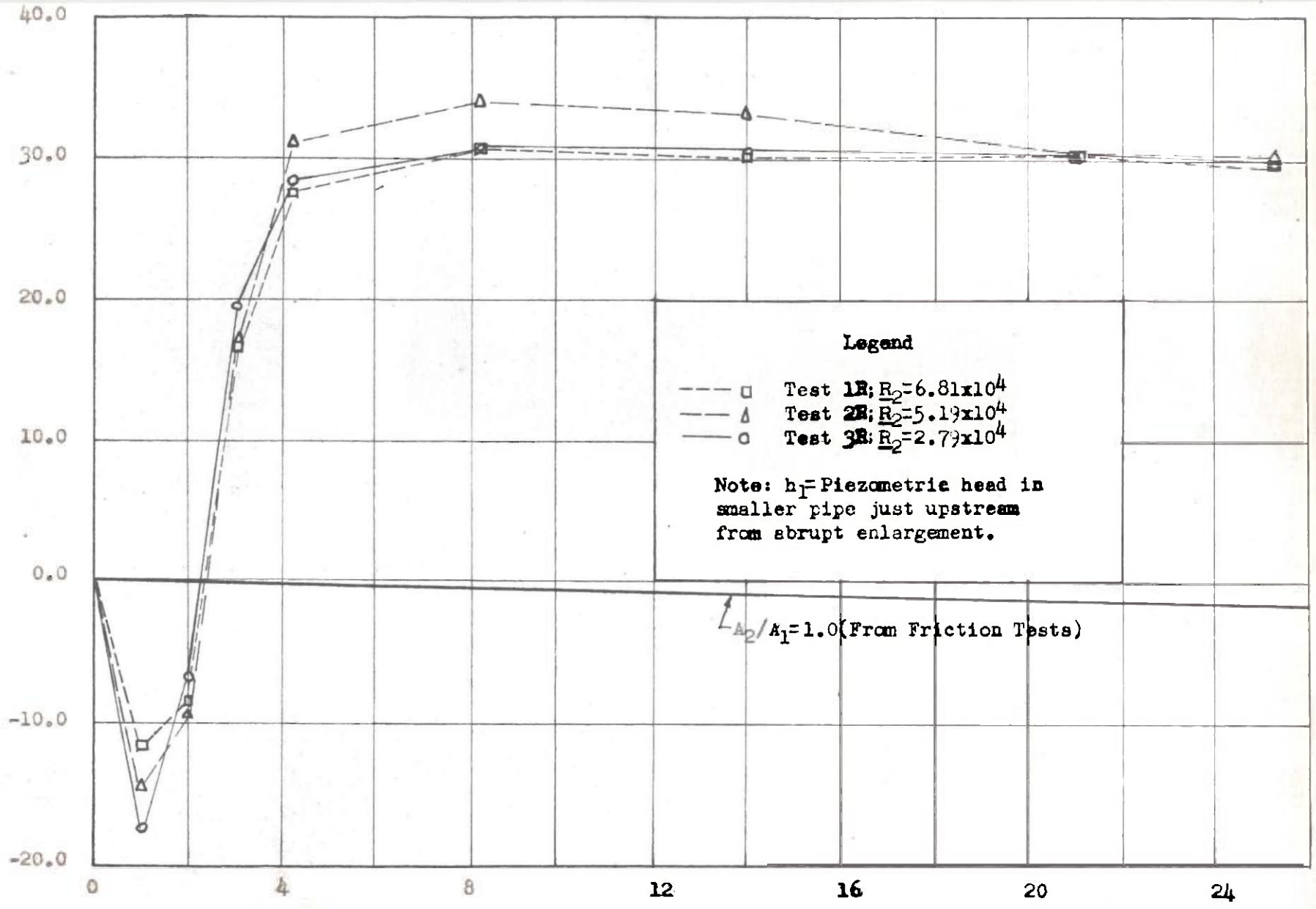

Fig.13. Piezometric Profiles, Rough Pipe, A_2/A_1=17.1

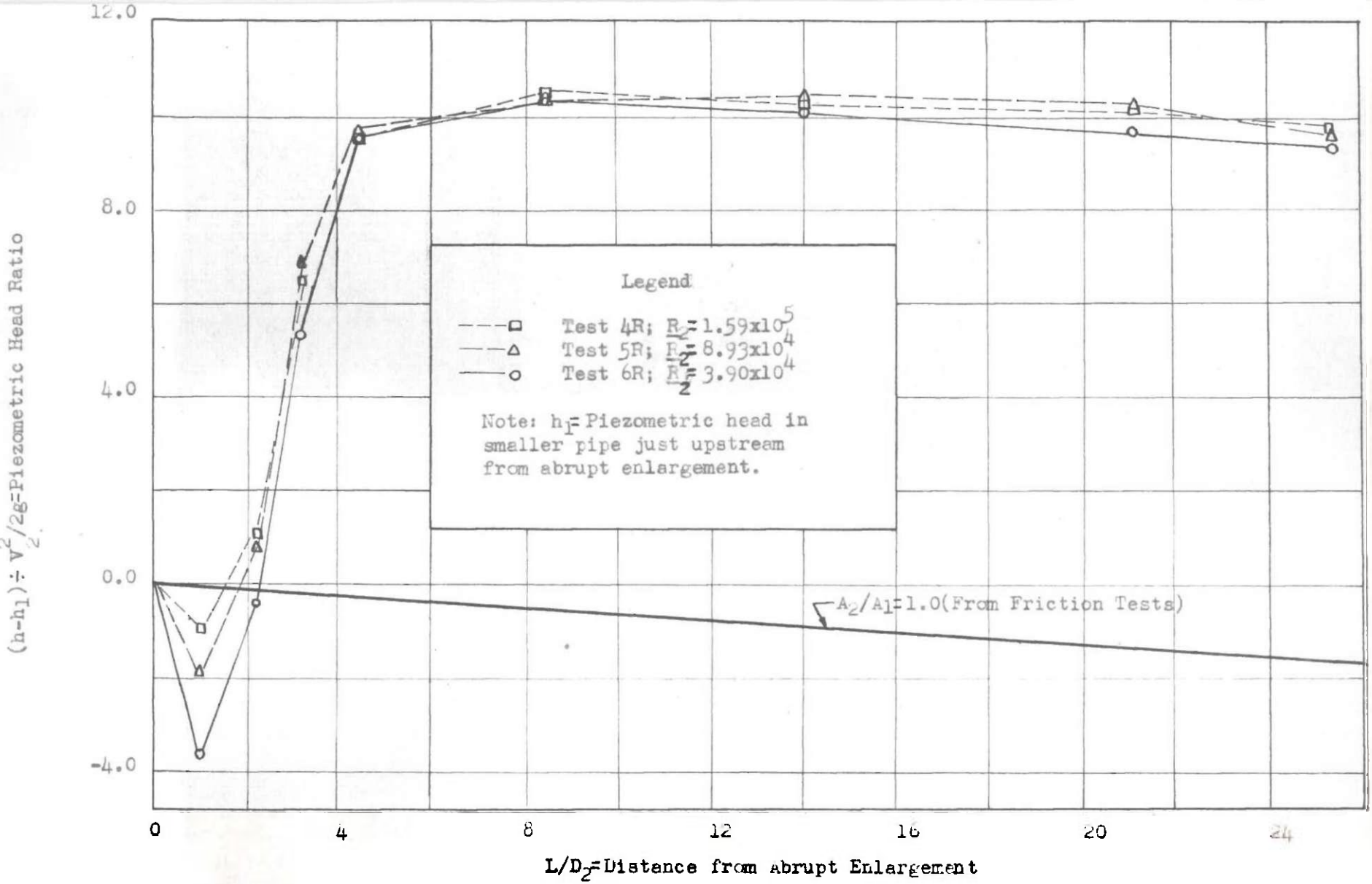

Fig.14. Piezometric Profiles, Rough Pipe, A_2/A_1=6.85

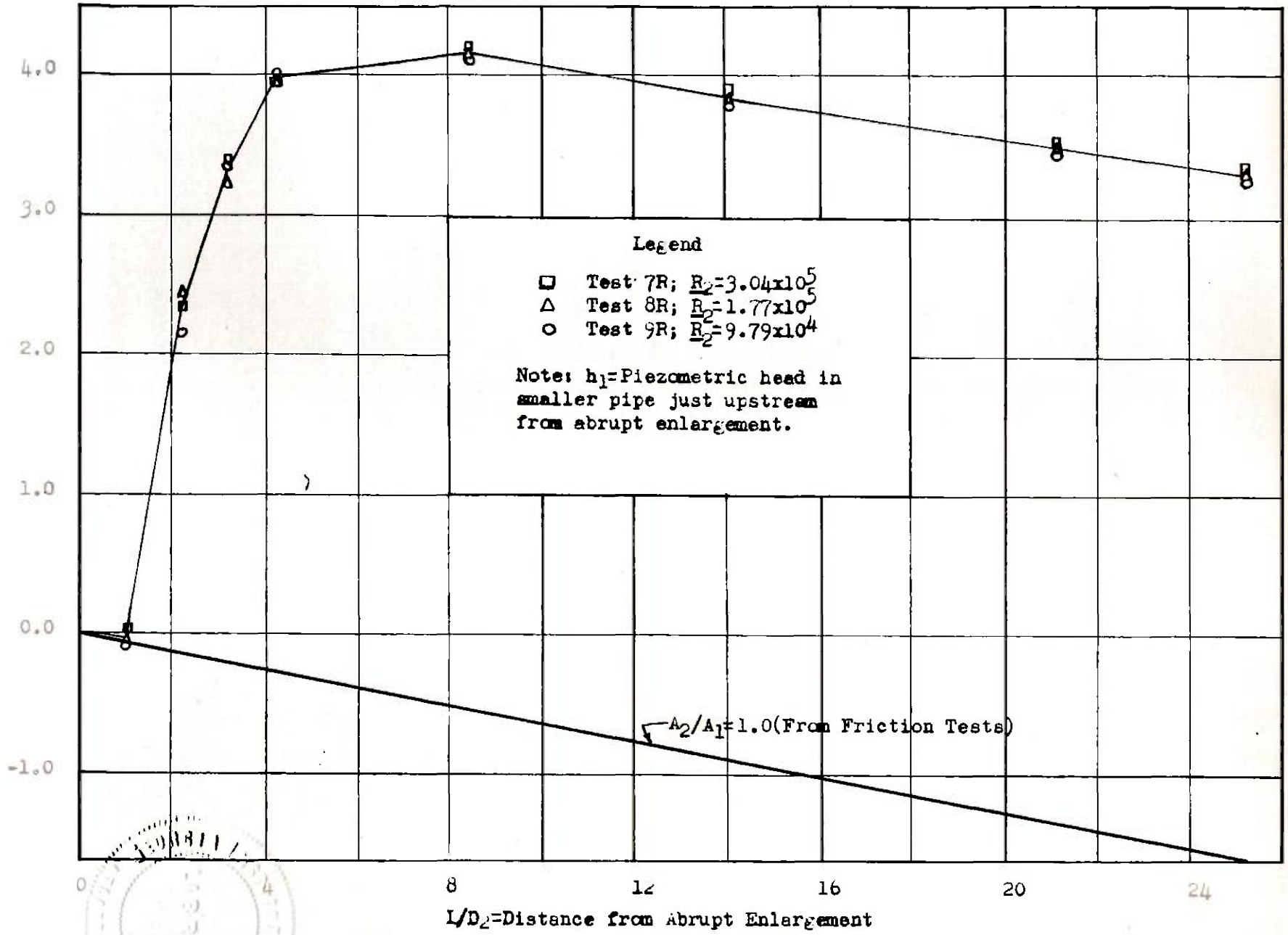

Fig.15. Piezometric Profiles, Rough Pipe, $A_2/A_1=3.34$

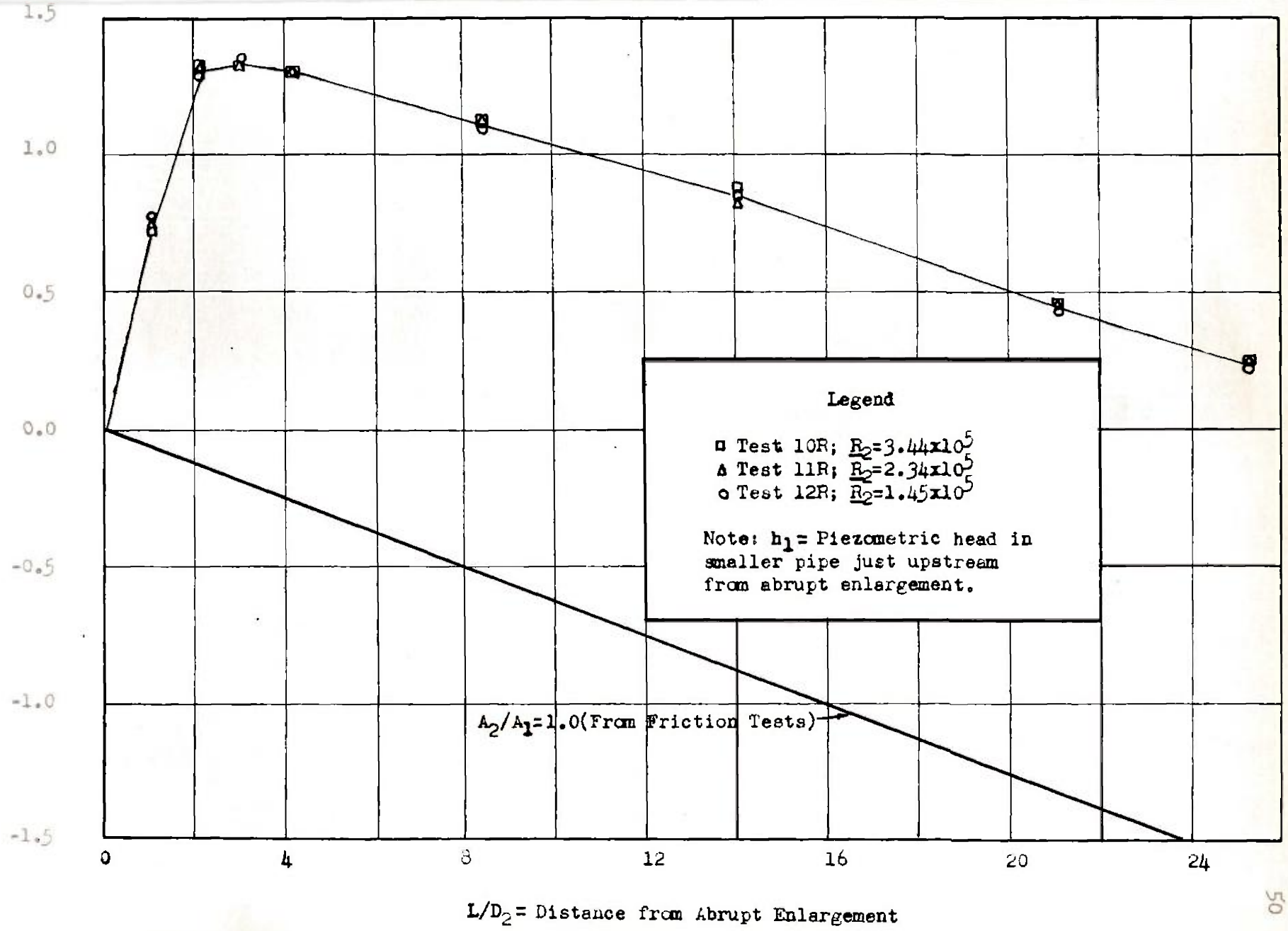

Fig.16. Piezometric Profiles, Rough Pipe, $A_2/A_1 = 1.82$

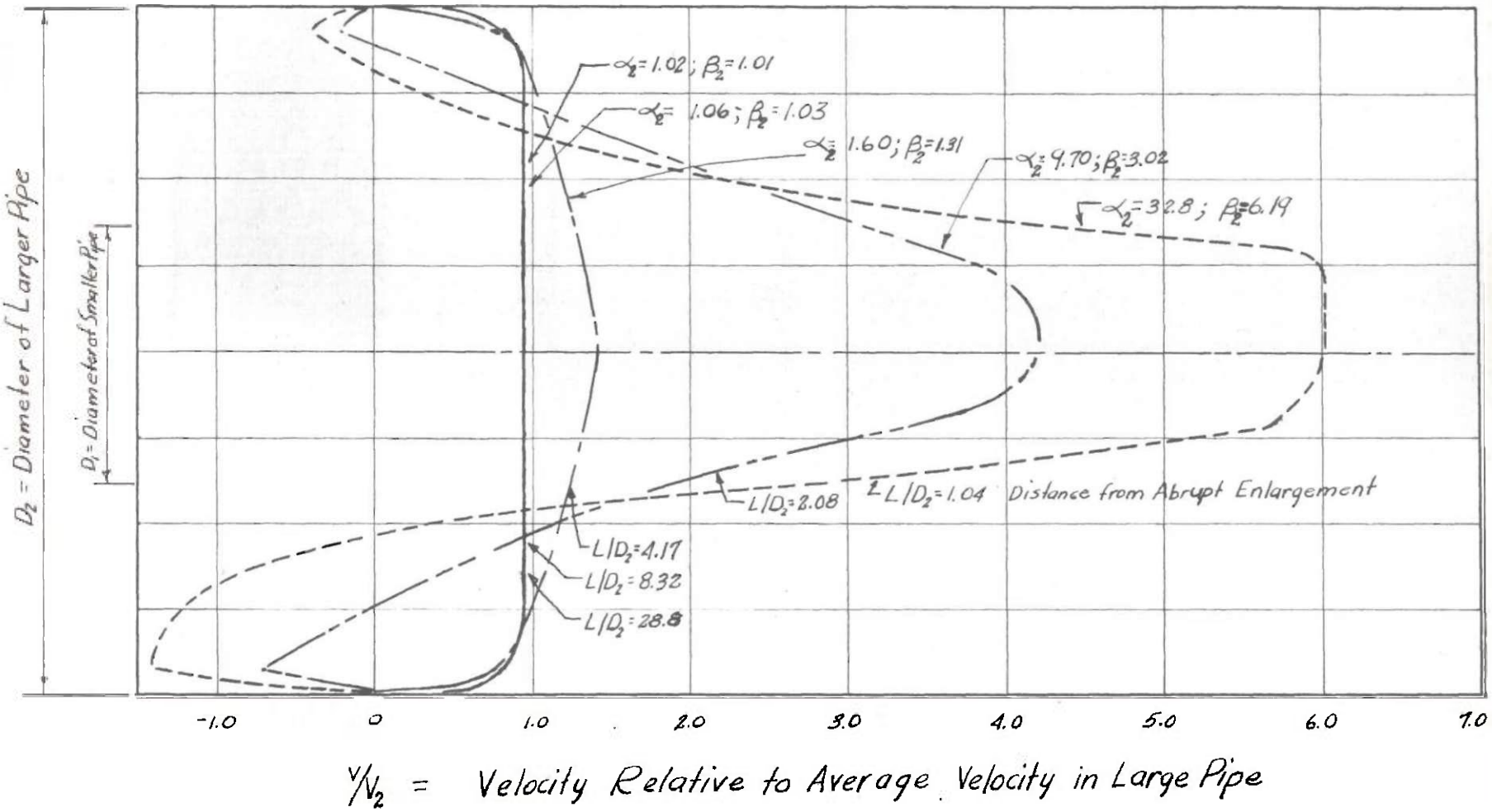

Fig.17. Velocity Profiles, Smooth Pipe, $A_2/A_1 = 7.01$, $R_2 = 1.21 \times 10^5$

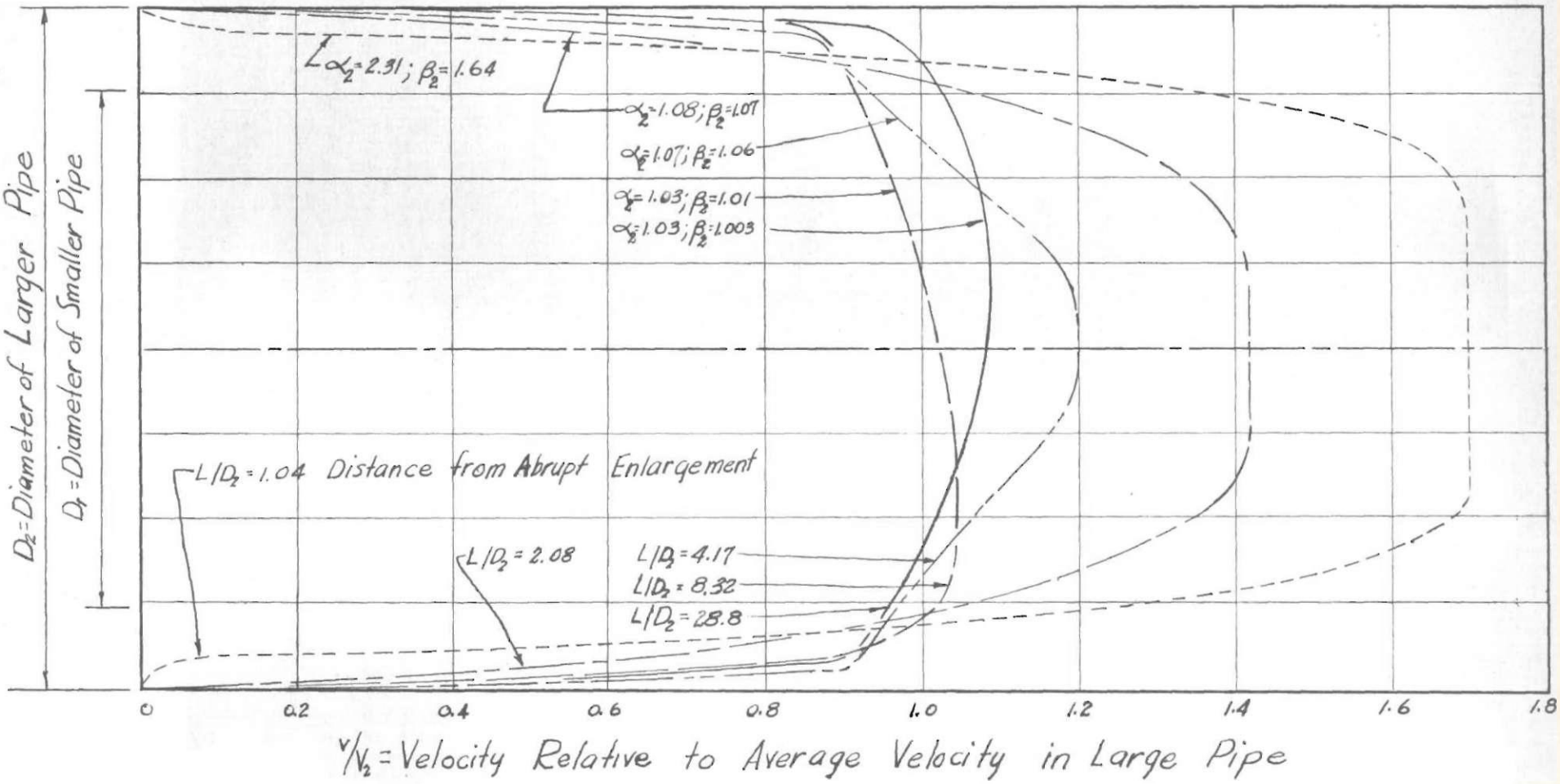

Fig.18. Velocity Profiles, Smooth Pipe, A_2/A_1=1.87, $R_{\underline{2}}$=2.60x10^5

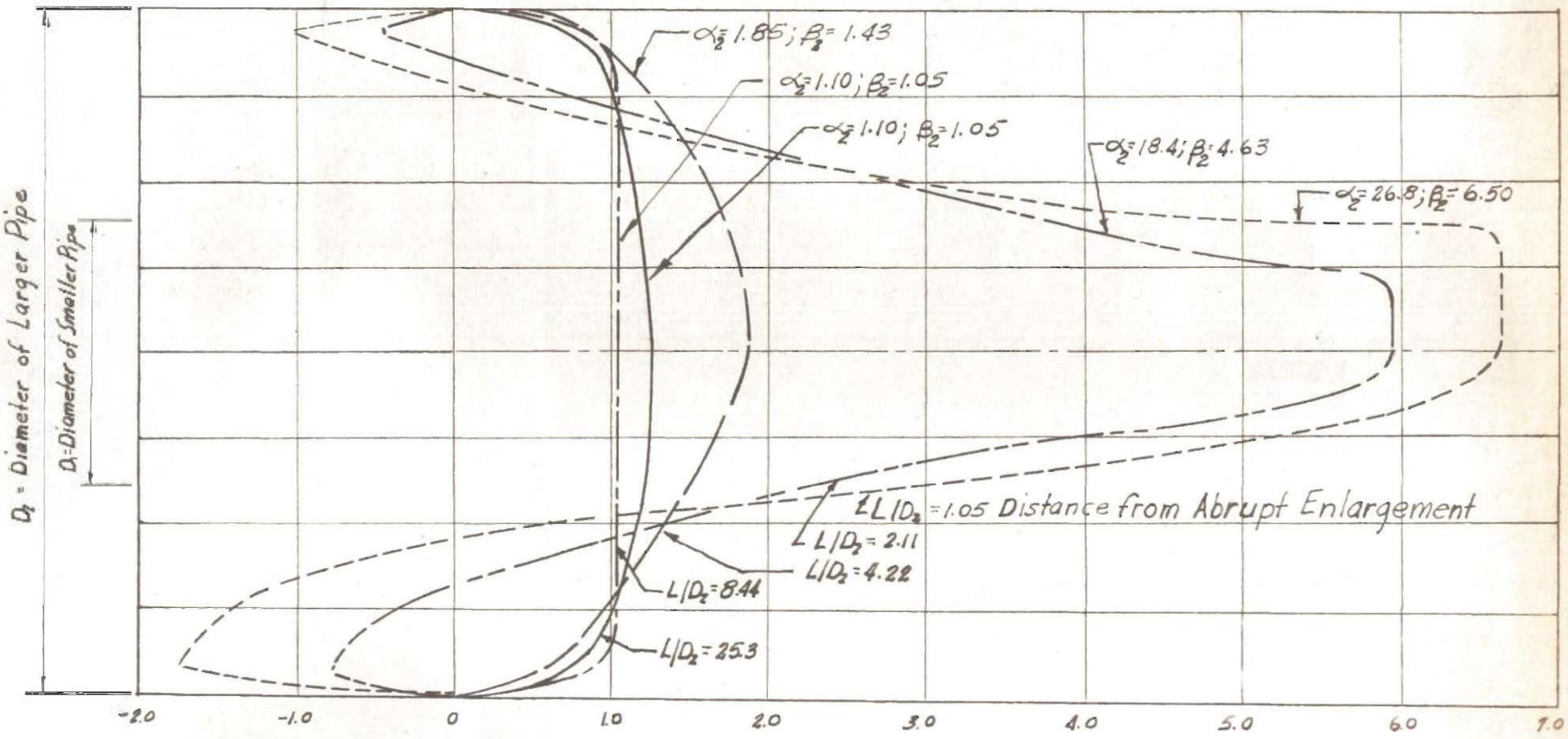

Fig. 19. Velocity Profiles, Rough Pipe, $A_2/A_1 = 6.85$, $R_2 = 1.21 \times 10^5$

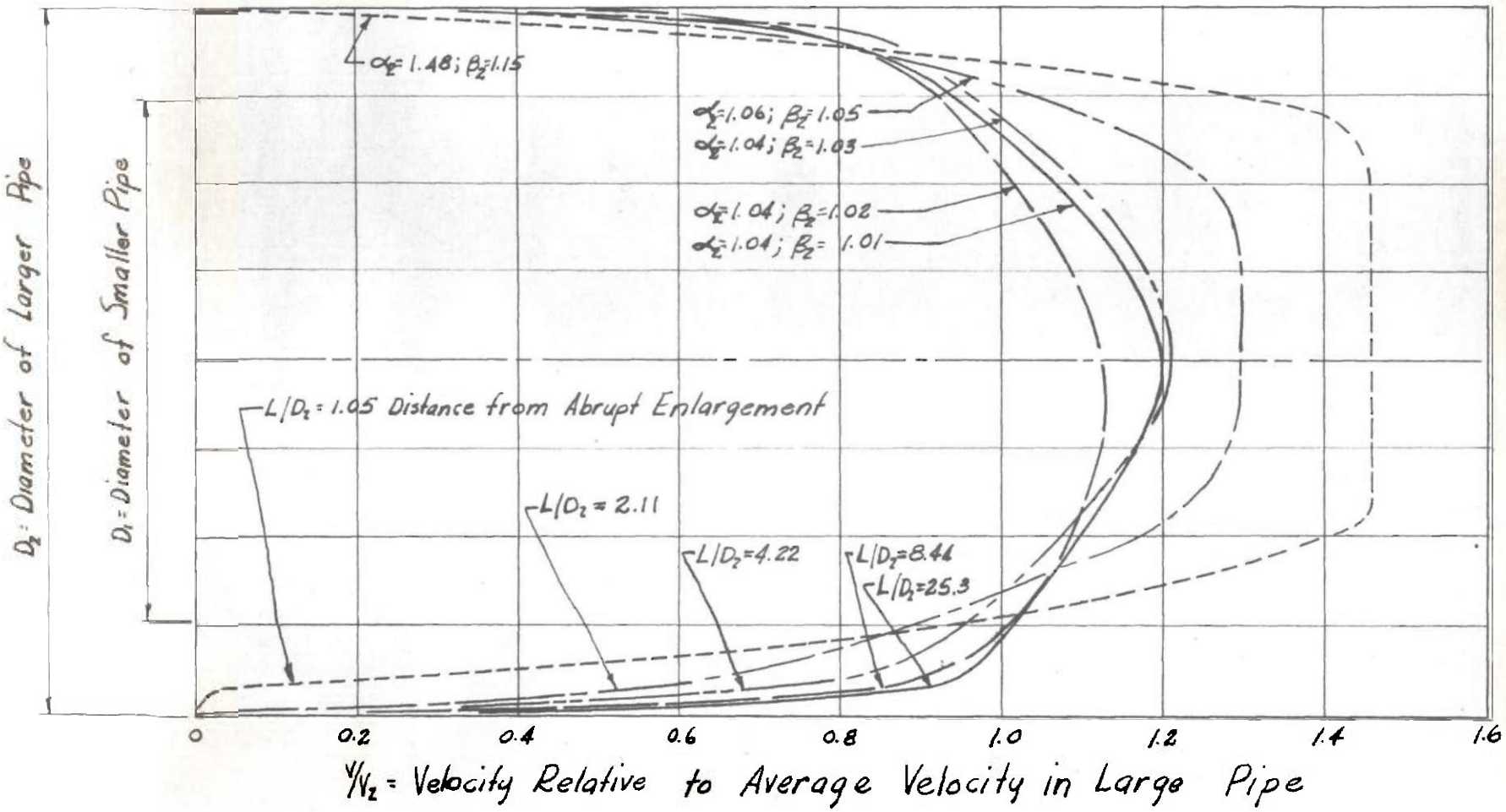

Fig.20. Velocity Profiles, Rough Pipe, A_2/A_1=1.82, R_2=2.54x10^5

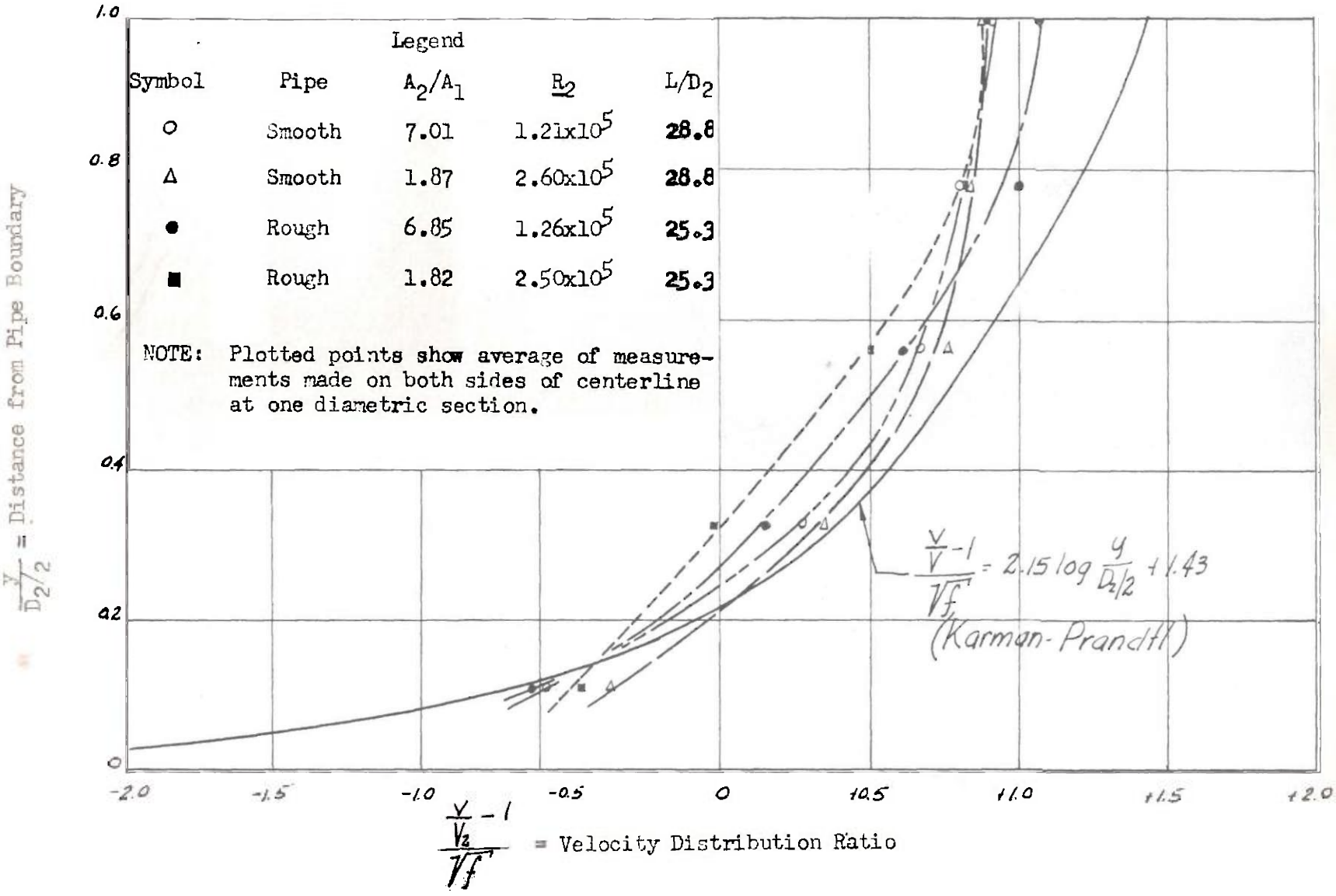

Fig. 21. Velocity Distribution at Downstream End of Pipe

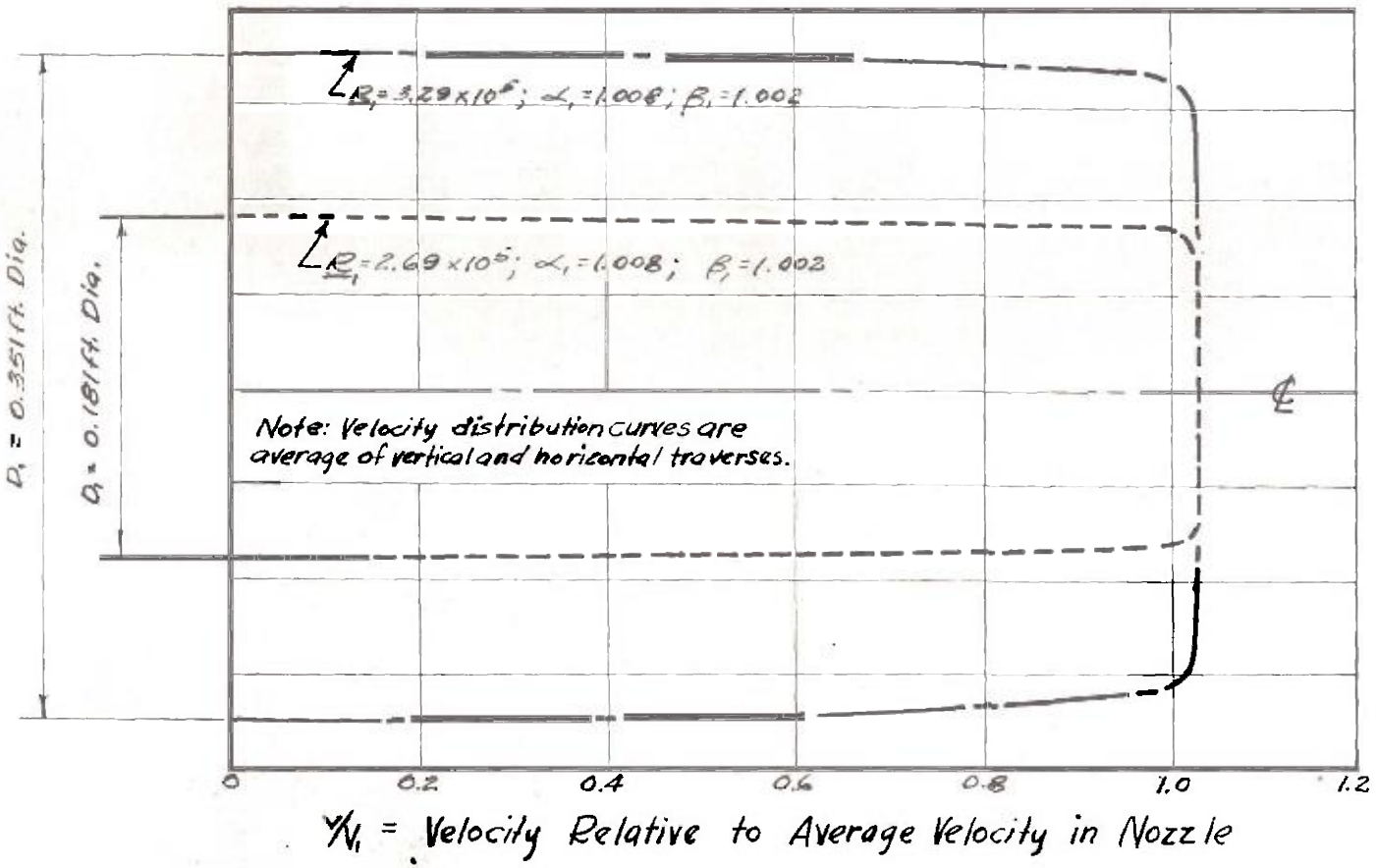

Fig. 22. Velocity Profiles in Two Nozzles

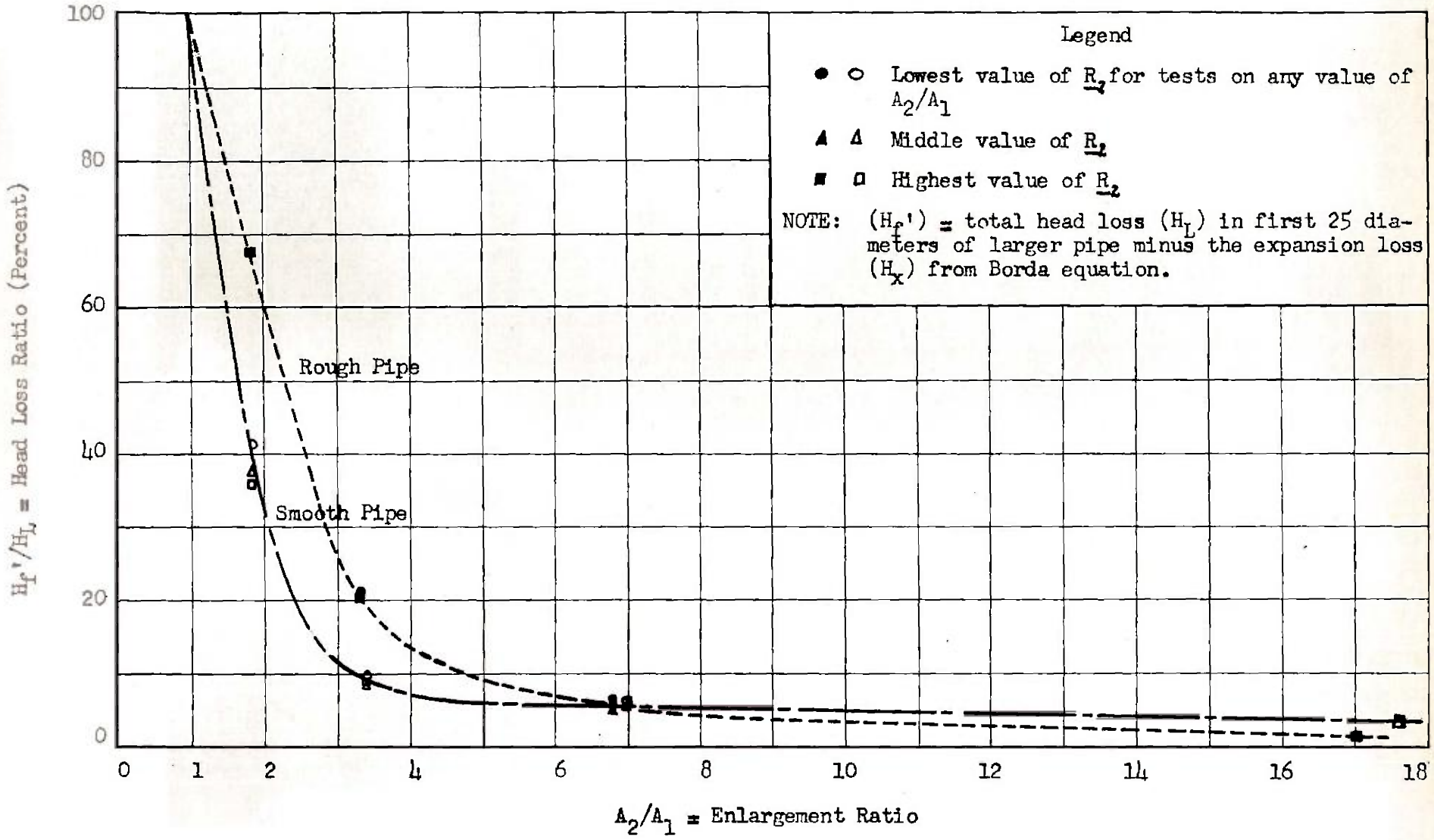

Fig. 23. Ratio of (H_f') to Total Head Loss

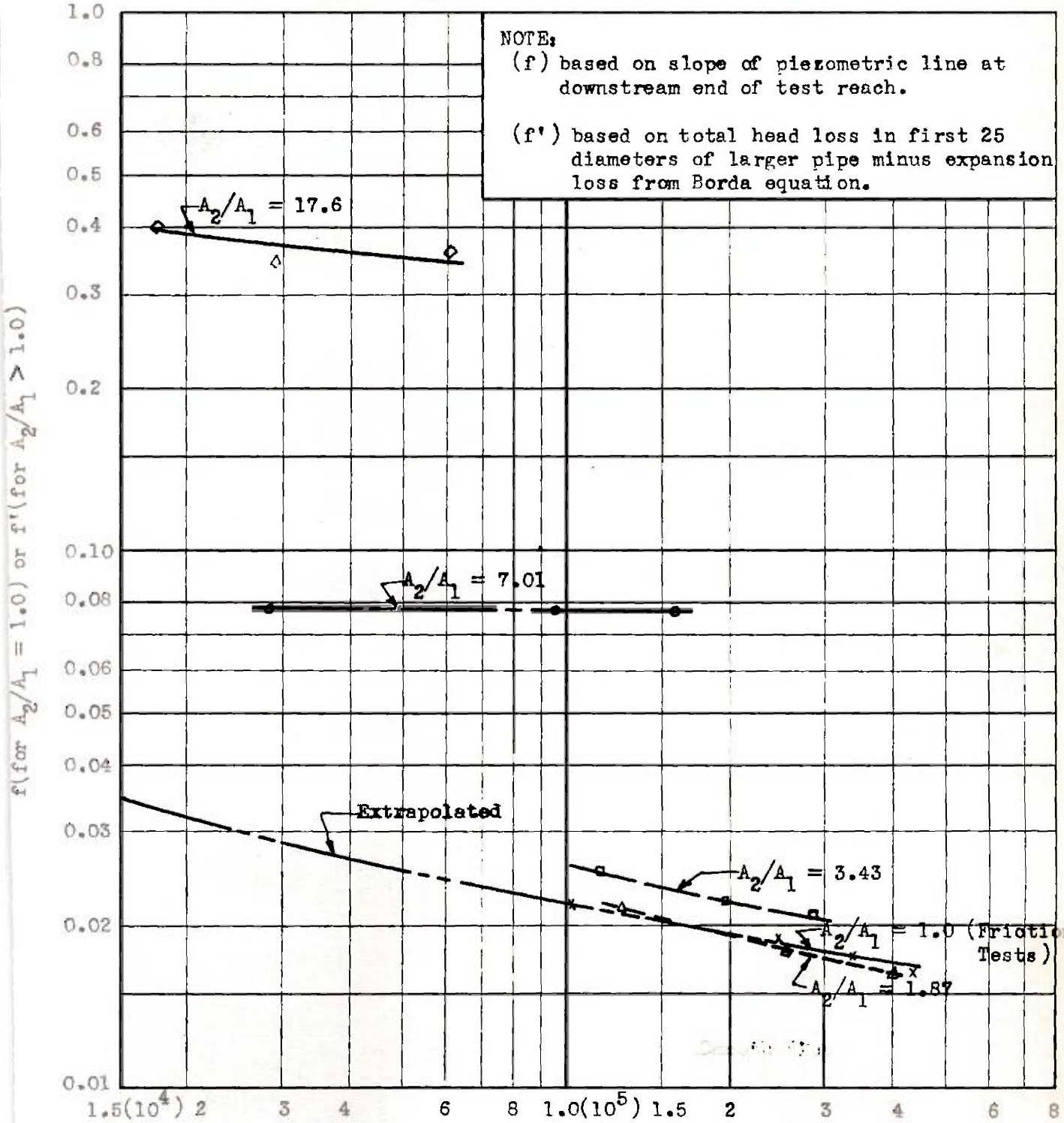

Fig. 24. Resistance Coefficients for Smooth Pipe.

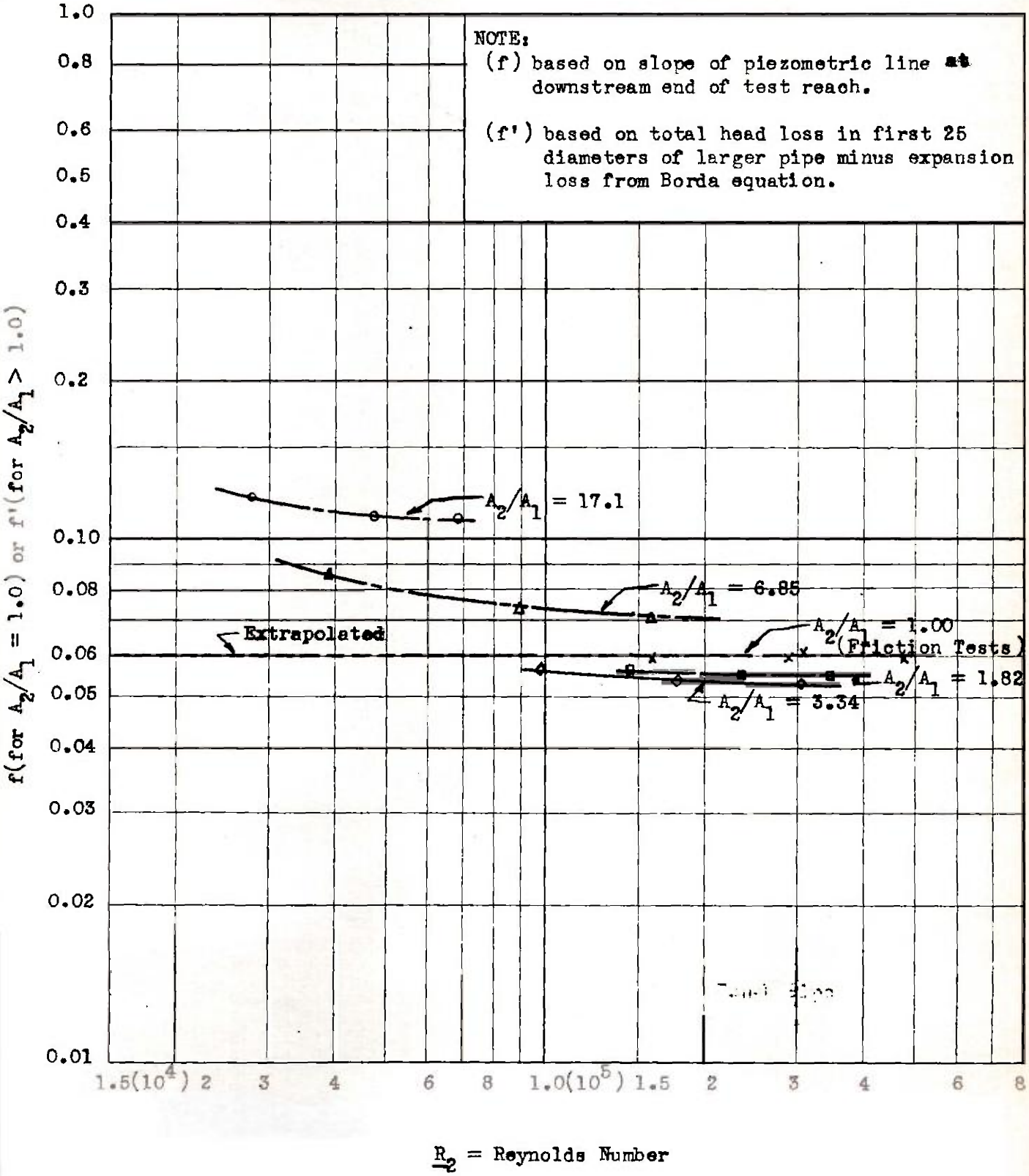

Fig. 25. Resistance Coefficients for Rough Pipe

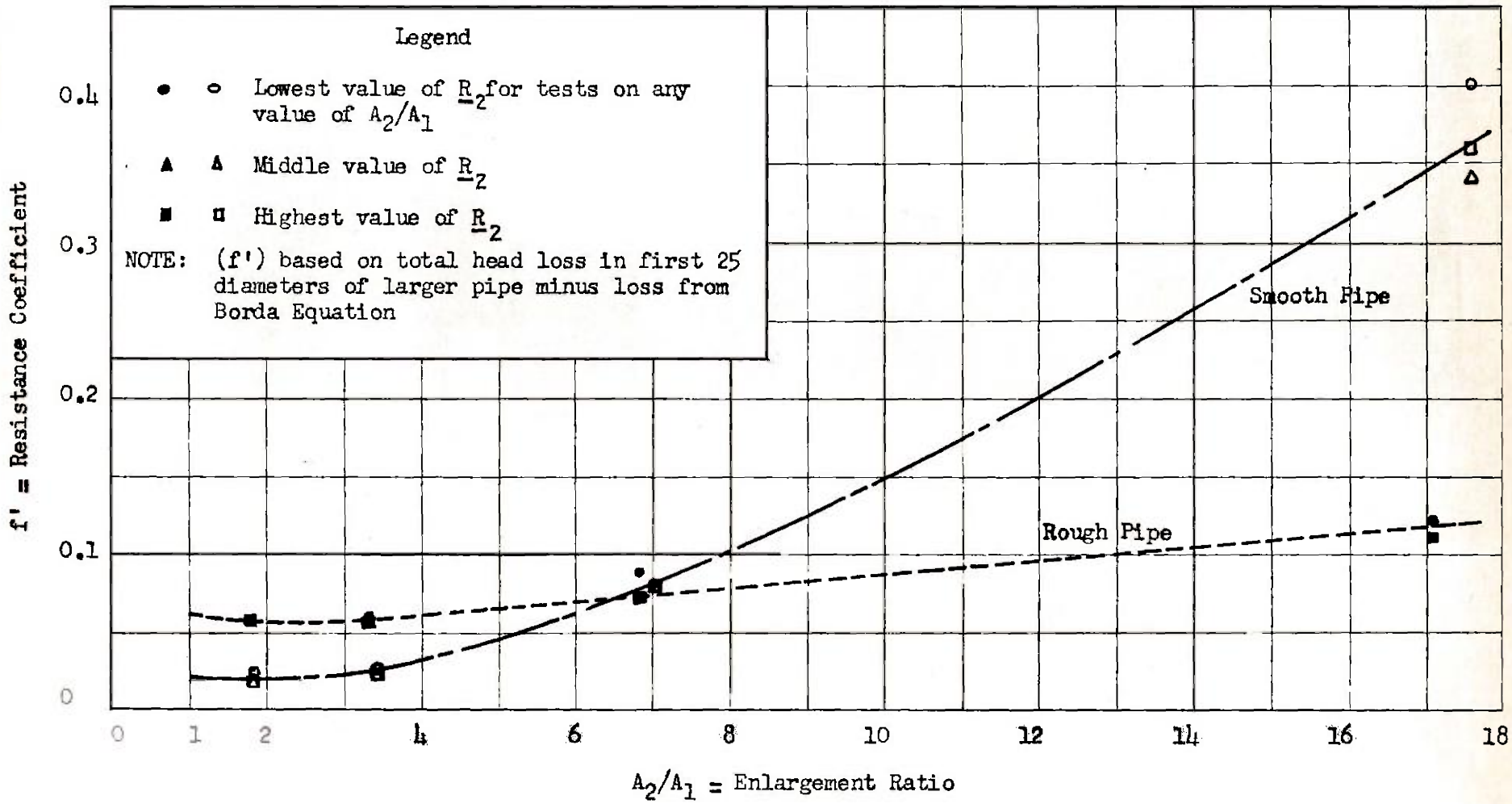

Fig. 26. Resistance Coefficient (f') for Abrupt Enlargements

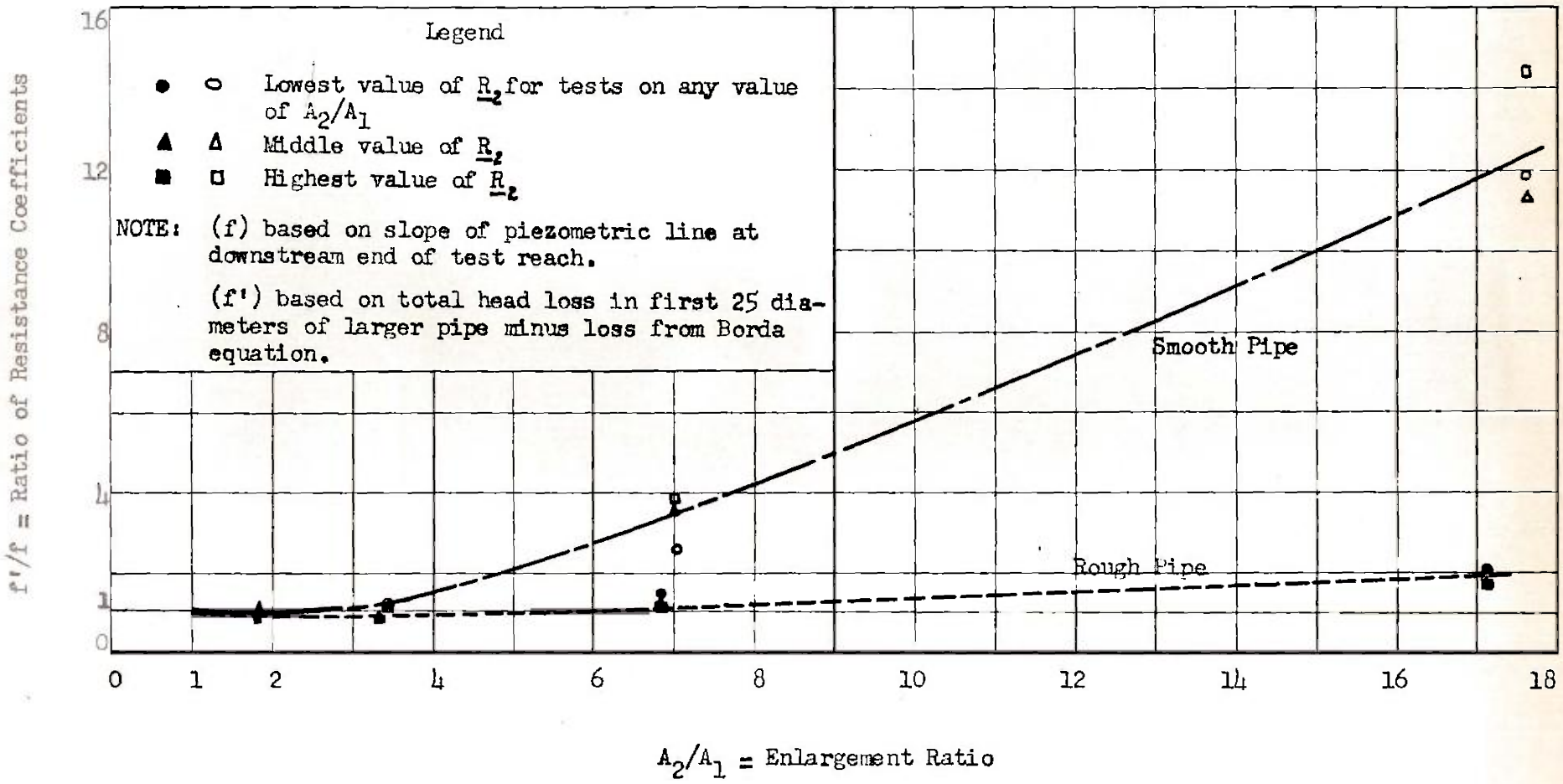

Fig. 27. Ratio of Resistance Coefficients, f'/f

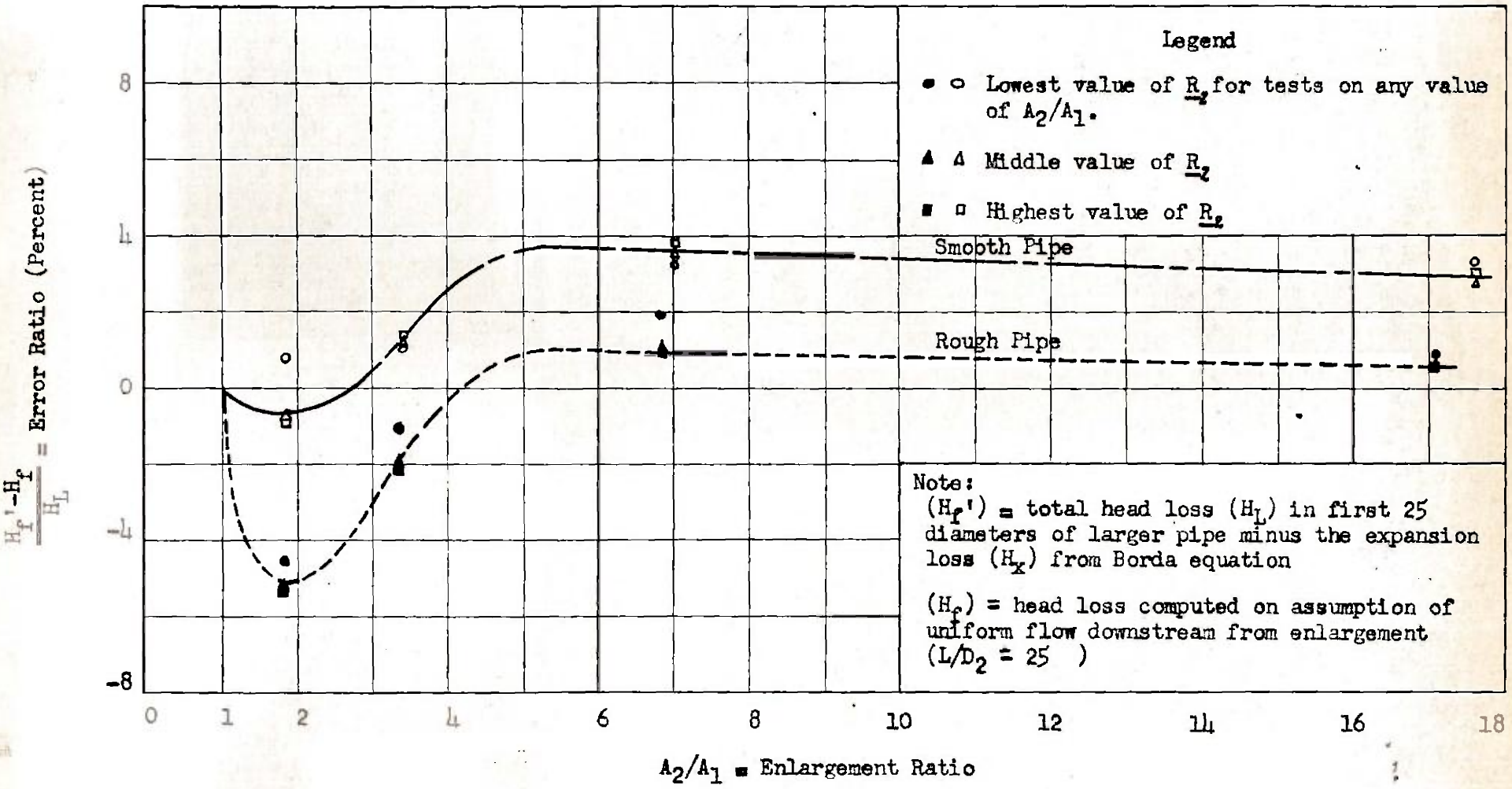

Fig. 28. Error in Assumption that $H_f' = H_f$.